의학박사 학위논문

Noradrenaline-mediated Differential Modulation of Cerebellar Module Activity during Locomotion

운동중 노아드레날린에 의한 소뇌 모듈 활성의 상이적 조절

2017년 8월

서울대학교 대학원

의학과 생리학 전공

허 성 원

A Thesis of the Degree of Doctor of Philosophy

운동중 노아드레날린에 의한 소뇌 모듈 활성의 상이적 조절

Noradrenaline-mediated Differential Modulation of Cerebellar Module Activity during Locomotion

August 2017

Department of Physiology
Seoul National University
College of Medicine

Sung Won Hur

Abstract

Noradrenaline-mediated Differential Modulation of Cerebellar Module Activity during Locomotion

Sung Won Hur
Department of Physiology
Graduate School
Seoul National University

The cerebellum is known for its role in maintaining coordinated motor movements. As the sole output of the cerebellum, the Purkinje cell (PC) is crucial for its role in gait, foot stride, limb trajectory, and balance. PCs were considered as homogeneous entities due to their cytoarchitecture, however, recent reports state that molecular identities and electrophysiological properties differ between zebrin II modules. Nonetheless, all cerebellar PCs have identical local synaptic circuits, as well as receiving noradrenergic inputs originating from the locus coeruleus (LC). The LC-noradrenaline (NA) circuit is active during motor behavior and give input to the cerebellum, but how NA contributes to cerebellar PC output and effect motor behavior remains unresolved. Here, we perform *in vivo* single-unit recordings of PCs from awake behaving mice along with pharmacological approaches and behavioral motion analysis to investigate how NA effects PCs across zebrin modules. Interestingly, we find that only PC modules expressing zebrin (Z+) have increased simple spike (SS) activity, while zebrin non-expressing (Z−) PCs have non-responsive

SS activity during locomotion. This modulation of PC SS output in Z+ modules during locomotion was insubstantial by destroying the LC terminal or by local inhibition of adrenergic receptors (ARs) in the cerebellum. However, behavioral motion analysis show that blocking the noradrenergic neuromodulation of SS activity across zebrin positive PCs disrupt forelimb stride motion in DSP-4 injected mice but not in mice which were given acute local topical application of adrenergic receptor antagonist cocktail. To investigate the mechanism of SS enhancement of Z+ PCs, we examined the effect of α_2-ARs on molecular layer interneurons (MLIs). Previous *in vitro* experiments have shown that MLIs contain α_1 and α_2-ARs which dual modulate MLI firing activity upon activation. *In vivo* MLI recordings from Z+ and Z− modules show that blockade of α_2-ARs does not alter the firing frequency during locomotion in comparison to control. Next, we examined the effects of ARs on PCs. Blocking α_2-ARs did not show any differences compared to control, but inhibition of β_2-ARs located on PCs may modulate the SS of PC output in Z+ modules. Altogether, these findings show that NA acts as a neuromodulator in the cerebellum which modulates SS output of PCs in Z+ modules possibly via β_2-ARs of PCs.

Key Words: Cerebellum, Noradrenaline, Purkinje Cell, Zebrin, Simple Spike Activity, Locomotion

Student Number: 2009 – 21857

CONTENTS

Abstract ····· **i, ii**

Contents ····· **iii**

List of Figures ····· **iv-vi**

Chapter I

Cerebellar-Noradrenergic Control on Locomotion

Introduction ····· **1**

I-1. Brief History of the Cerebellum ····· **1**

I-2. The Architecture of the Cerebellum ····· **2**

I-3. Cerebellum on Locomotion ····· **4**

I-4. The Locus Coeruleus – Cerebellum Circuit ·· **5**

I-5. Scope of Thesis ····· **6**

Chapter II

Noradrenaline-mediated Differential Modulation of Cerebellum Module Activity during Locomotion

Materials and Methods ····· **8**

Results ····· **12**

Discussion ····· **68**

References ····· **76**

Abstract (Korean) ····· **85, 86**

LIST OF FIGURES

Figure 1. The involvement of the cerebellum in the control of locomotion behavior • 22, 23

Figure 2. *In vivo* PC recording configuration and motion tracking in awake mice • 24, 25

Figure 3. Post-hoc identification of recorded PC site and Aldolase C/ Zebrin II • 26, 27

Figure 4. Zebrin-dependent SS and CS activity during quiet wakefulness state in awake mice • 28, 29

Figure 5. Behavioral state-dependent differential activity of PCs • • • • • 30, 31

Figure 6. Increased simple spike activity of Z+ PCs during locomotion • 32, 33

Figure 7. Change in simple spike firing patterns during locomotion in Z+ PC • 34, 35

Figure 8. Z+ and Z− PC firing activity upon reduction of noradrenergic input via DSP-4 • 36, 37

Figure 9. DSP-4 disrupts noradrenergic modulation of Z+ PC activity during locomotion • 38, 39

Figure 10. Abnormal limb motion in DSP-4 injected mouse • • • • • • • • • • 40, 41

Figure 11. Drug diffusion through the cerebellar cortex • • • • • • • • • • • • • 42, 43

Figure 12. The effect of local and direct inhibition of adrenergic receptors on Z+ PC activity • 44, 45

Figure 13. Local inhibition of noradrenaline input by adrenergic receptor antagonist cocktail reduces enhancement of Z+ PC simple spike activity • 46, 47

Figure 14. The effect of local and direct inhibition of adrenergic receptors on Z− PC activity • 48, 49

Figure 15. Inhibition of noradrenaline has no effect on Z− PC firing activity • 50, 51

Figure 16. No difference in forelimb motion upon application of adrenergic receptor antagonist cocktail • 52, 53

Figure 17. Inhibition of α2-adrenergic receptors on molecular layer interneurons of Z+ modules • 54, 55

Figure 18. Inhibition of α2-adrenergic receptors on molecular layer interneurons of Z− modules • 56, 57

Figure 19. Blockage of α2- adrenergic receptors during locomotion in Z+ PC • 58, 59

Figure 20. Blockage of α2-adrenergic receptor has no effect on PC simple spike activity • 60, 61

Figure 21. Effect of β2-adrenergic receptors by ICI 118, 551 on Z+ PC activity • 62, 63

Figure 22. Inhibition of β2-adrenergic receptors block enhancement of simple spike activity of Z+ PCs • 64, 65

Figure 23. Conclusion summary: Noradrenergic effect on zebrin II-dependent PC SS activity and behavior, and its possible mechanisms • • • • • • • • • • • 66, 67

CHAPTER I

Cerebellar-Noradrenergic Control on Locomotion

Introduction

I – 1. Brief History of the Cerebellum

The cerebellum derives its term as a miniature of the word "cerebrum". The first description of the cerebellum was provided by Galen (AD 126 – c. 210) as a source of motor function in association with the spinal cord (Elhadi et al., 2012). In the 18th century, more accurate anatomical descriptions of the cerebellum started to emerge (Glickstein et al., 2009). One of the first work solely on the cerebellum itself was by Malacarne (1744 – 1816) in 1776 (Cherici, 2006) and by the end of the 18th century, an accurate picture of the gross anatomy of the cerebellum had been established.

Although there were speculations about the function of the cerebellum, it is not until the 19th century that experimental approaches were done in animals which gave more accurate functional understanding of the cerebellum (Glickstein et al., 2009). Pierre Flourens (1794 – 1867) found through his experiments that the ablation of the cerebellum showed discoordination and concluded that the coordination of movements resides in the cerebellum, which remains effective today (Pearce, 2009). Clinically Gordon Holmes (1876 – 1965) reported that cerebellar damage showed symptoms like, hypotonia, asthenia, tremor, vertigo, ataxia, and disturbance in gait and balance (Holmes, 1917).

I – 2. The Architecture of the Cerebellum

Since the first description of the Purkinje cell (PC) of the cerebellum by Jan Evangelista Purkinyě (1837) and a more detailed depiction of the cerebellar neuronal architecture by Ramón Cajal (1909), many studies have provided information on the structures and cells that form the cerebellar cortex.

Macroscopically, the cerebellum cortex consists of two hemispheres adjoined by the vermis in the middle. The vermis consists of ten lobules which can be divided into three lobes: the anterior (lobules I-V) and posterior (IV-IX), which are separated by the primary fissure, and the floccculonodular lobe (lobule X, paraflocculus and flocculus) separated by the posterolateral fissure.

Each lobule of the cerebellar cortex is divided in to three layers. Starting from the surface of the cortex, the molecular layer, Purkinje cell layer, and granule cell layer (Figure 1A). In these well-organized layers, there are many types of cells which converge its information onto one type of cell: The Purkinje cell. The PC is the sole output of the cerebellar cortex, which receives two main excitatory inputs: the parallel fiber (PF) input originating from the granule cells (GrC) of the granule cell layer and the climbing fiber (CF) input from the inferior olive (IO) of the brainstem. Additionally, the PC receives inhibitory inputs mainly by molecular layer interneurons (MLIs). Theses inputs are processed by the PC and expressed as simple spikes (SSs), PF and MLI inputs, which fires irregularly at a high-rate (17 – 150 Hz), and complex spikes (CSs), CF inputs, which has multi-peaks and fires at a low frequency firing rate (1 – 2 Hz).

The PCs of the cerebellum has been known for its uniform cytoarchitecture. Until recently, PCs have been considered as a homogeneous entity due to the uniform structure and connectivity. However, reports have shown that this is not the case (Zhou et al., 2014, Jelitai et al., 2016).

Zebrin II/ aldolase C, a PC marker, are expressed as parasagittal stripes in the cerebellum. Starting from the midline, zebrin II expressing (Z+) PCs in the vermis are labeled from P1+ through P4+ and zebrin non-expressing (Z−) PCs are labeled P1- through P3- which are adjacent to each other forming stripe patterns.

The functions of these zebrin II stripes are still unknown. However, these alternating stripes of zebrin II PC modules have been reported to have different basal PC activity in awake mice (Zhou et al., 2014). In addition, reports have shown that various proteins involved in cellular activity and memory formation are also expressed as parasagittal stripes, such as GABA receptors (Chung et al., 2008), type 1 inositol 1, 4, 5-triphosphate receptor (Furutama et al., 2010), phospholipase C (Sarna et al., 2006), protein kinase C (Barmack et al., 2000), mGluRs (Mateos et al., 2001), and the excitatory amino acid transporter 4 (Dehnes et al., 1998). How these molecules are in relation to zebrin II is yet unclear.

In relation to parasagittal zebrin II patterns, tracing and immunohistochemistry studies have shown that mossy fiber and climbing fiber inputs also show projection patterns in which it corresponds to zebrin II expression (Quy et al., 2011, Gebre et al., 2012, Voogd et al., 2003). Thus, the similarity of projection zones and zebrin II expression may have functional

implications when compared during motor behavior.

I – 3. Cerebellum on Locomotion

The decision of locomotor behavior involves regions of the basal ganglia, hypothalamus, and thalamus which projects to the motor cortex and other regions of the cortex (Figure 1B). This information is then conveyed to the mesencephalic locomotor region to initiate locomotion. These neurons project to the reticular formation of the brainstem which then projects to the spinal cord to execute locomotion. The role of the cerebellum in locomotor behavior is to monitor rhythmic activity of the central pattern generator of the spinal cord and send feedback via the deep cerebellar nucleus, which projects back to the brainstem to modulate the ongoing activity of the central pattern generator to adjust to changing environment.

Since that the cerebellum manages acquisition and performance of accurately timed and smooth coordinated movements, damage of the cerebellum is well-known to cause deficits in gait, foot length, limb trajectory, and balance (Thach et al., 1992, Welsh et al., 1995, Machado et al., 2015, Kiehn, 2016).

Cerebellar and inferior olive lesion studies suggest that most parasagittal modules are involved in locomotion in a specific manner. Midline modules of the cerebellum regulate balance by controlling tone of the extensor muscles (Mori et al., 1999, Pijpers et al., 2008). Clinical studies of patients with olivocerebellar lesions also show that medial zones affect balance and gait

(Morton and Bastian, 2007, Ilg et al., 2008). In addition to contribution of olivocerebellar pathway to locomotor behavior, mossy fiber pathways which give different inputs to parasagittal modules of the cerebellum, also show a representation of the forelimb motion during locomotion (Powell et al., 2015).

I – 4. The Locus Coeruleus – Cerebellum Circuit

Aside from synaptic inputs that form the cerebellar local circuit, the cerebellum receives noradrenergic inputs originating from the locus coeruleus (LC) (Abbott and Sotelo, 2000, Paukert et al., 2014). LC axons stretch out to almost all areas of the brain which its mostly open axon terminals transmits noradrenaline (NA) through volume transmission (Bloom et al., 1971, Olson and Fuxe, 1971, Abbott and Sotelo, 2000, Sara, 2009, Schwarz and Luo, 2015, Foote et al., 1983).

The activation the noradrenergic circuit have been shown to effect locomotor activity (Carter et al., 2010), as well as having functional roles in pain modulation (Sugiyama et al., 2012), sleep, attention, arousal, and motor behavior (Rommelfanger et al., 2007).

The cerebellum contains α_1, α_2, β_1 and β_2- adrenergic receptors (ARs). *In vitro* cerebellar slice studies have shown that α-ARs and β-ARs have a bidirectional effect on PC synaptic and firing activity while NA has an depressive effect on PC activity (Parfitt et al., 1988, Hirono and Obata, 2006, Lippiello et al., 2015).

Also, *in vivo* experiments under anesthesia have shown that PC

activity decreases by NA release via LC electrical stimulation (Bickford-Wimer et al., 1991) or direct application of NA (Guo et al., 2016). Awake *in vivo* studies have shown that α_2-AR knockout mice had impaired locomotion activity and motor coordination (Lahdesmaki et al., 2002). However, how noradrenergic inputs effect cerebellar output in awake behaving animals has yet to be described.

I – 5. Scope of Thesis

The current study focuses on mainly three purposes: First, how heterogeneous zebrin II expressing and non-expressing PCs with different basal outputs are modulated during locomotion. Second, to investigate whether noradrenergic input affect differently modulated heterogeneous PCs during locomotion. Despite that previous studies which investigated the *in vivo* noradrenergic effect on PCs, these studies were done anesthesia which have been proven to have different PC SS firing properties to that of awake mice in vivo (Shin et al., 2007). In addition, a recent report states that activity recordings of PCs in awake *in vivo* mice are bidirectionally modulated during locomotion due to the balance in dendritic excitation-inhibition (Jelitai et al., 2016). Nevertheless, how NA contributes to cerebellar PC output and effect motor behavior remains unresolved. Third, the mechanism on what circuit or which AR noradrenaline effects to give differently modulated PC output.

Here, I hypothesize that PCs within different zebrin modules may have distinct firing activity during motor behavior in accordance to the effect of NA

in the cerebellum. To test this hypothesis, I performed *in vivo* single-unit recording in the cerebellum of awake behaving mice to record simple and complex spiking of PCs along with forelimb motion analysis during locomotor behavior. Pharmacological approaches were used to investigate the effect and mechanism of NA in the cerebellum and how it affects locomotion.

CHAPTER II

Noradrenaline-mediated Differential Modulation of Cerebellum Module Activity during Locomotion

Materials & Methods

Animals

Male 7-10 week-old, C57BL/6J mice were used during all experiments. Mice were kept in a group of two to five animals per cage and kept in 12 h light/dark cycle. Food and water were available *ad libitum*. All animal experiments were approved by the Seoul National University Institutional Animal Care and Use Committee.

Surgeries

In preparation for recordings of *in vivo* awake mice, an incision of the skin over the skull was made over the rostocaudal mid-line. Then a lightweight head-ring (0.5g) was attached to the skull using Superbond dental cement (Sun Medical, Japan). All surgeries were done under 2.5% isoflurane anesthesia. After 3 days of recovery, ~1.5 mm x 1 mm craniotomy was made directly above lobule V of the cerebellum. The craniotomy was sealed with 2% agar and placed on the recording set for ~1h to recover from anesthesia.

In vivo Single-Unit Recordings

Head posted mice were handled and habituated to the recording experimental setup 3 days prior to recording. Before every recording session, mice underwent handling for 5 mins. Head posted mice were able to walk, run or sit on the cylindrical treadmill. Single-unit recordings were done using 5-7 MΩ borosilicate glass pipettes (WPI, FL, USA) filled with 2 M NaCl and 2 µl/ml hoechst 33342 was added before recording. External solution applied during the recordings contained 135 mM NaCl, 2.7 mM KCl, 1 mM $MgCl_2$, 5 mM $CaCl_2$, and 5 mM HEPES, (pH adjusted to 7.4 with NaOH). Using a one-axis micromanipulator (Narishigae, Japan), PCs and MLIs were identified by their firing characteristics and depth from the pial surface (PC: 200 – 250 µm; MLI 0 - 200 µm). Recordings were amplified and filtered 300-5 kHz using A-M systems model 1800 amplifier (A-M systems, USA) and data was digitized at 10 kHz using pClamp 10 software via DigiData 1440 (Molecular Devices, USA). After successful recordings, a brief air-puff was given to mark the recording site. For *post-hoc* immunohistochemistry, mice were anesthetized with 10% urethane (1.5 mg/kg) and the brain was extracted after mice were transcardially perfused with 4% paraformaldehyde.

Drugs

For N-(2-chloroethyl)-N-ethyl-2-bromobenzylamine (DSP-4) experiments, drug was administered via i.p. injection (50 mg/kg) 7 days prior to recording experiments. To block noradrenergic receptors, α_1, α_2, β_1, and β_2

noradrenergic receptor antagonists (1 mM prazosin, yohimbine, betaxolol, and ICI 118,551) were mixed in external solution (pH 7.3). The noradrenergic receptor blocker cocktail was applied topically to lobule IV/V recording window and recordings were done >5 min after application. All drugs were dissolved in 0.9% NaCl for i.p. injection or external solution for topical application.

Immunohistochemistry

Post-transcardial perfusion, each brain was submerged in 4% paraformaldehyde overnight. Coronal sections (50 μm) were made using a vibratome (Leica VT1000S) in phosphate buffered solution (PBS). For zebrin staining, slices were washed and transferred to a slide glass. After permeabilization with PBSTx (0.3% Triton X-100 in PBS), sections were incubated in blocking solution (20% normal goat serum in PBSTx) for 1 h and washed with PBSTx. Rabbit derived Aldolase C/ Zebrin II (1:500, Frontier Institute Co. Ltd, Japan) primary antibody and anti-rabbit Alexa 594 (1:200, Sigma) secondary antibody was used to stain the zebrin positive PCs. Sections were mounted using mounting media which were covered with a cover glass for analysis.

Behavioral Motion Tracking

Behavioral movements were analyzed on-line and visually recorded (32 f.p.s.) using a digital camera (IMPERX, USA), infrared (IR) light, and

custom made motion tracking software (LabVIEW). An infrared (IR) reflective sticker was placed on top of the scapula bone or paw of the right forelimb to track forelimb motion.

Data Analysis

Spike detection was done via mini-analysis (Synaptosoft). Simple and complex spikes were discriminated manually and were rechecked by 2 different people. Frequency data, CV2 data were analyzed by using a custom made software (LabVIEW) to align it to motion data. All data were process and analyzed in statistical software Origin 9.0 (OriginLab).

Results

To investigate the output of Z+ and Z- PCs during locomotion, I made single-unit recordings from PCs in lobule V of the cerebellar cortex of awake, head-fixed adult C57BL/6J mice (Figure 2A). Cerebellar lobule IV/V signify sensation and motor movement of limbs (Ozden et al., 2012, Hoogland et al., 2015, Sauerbrei et al., 2015, Jelitai et al., 2016). Once head-fixed mice were rested in quiet wakefulness state, an air-puff was given to induce locomotive activity (Figure 2A). Along with *in vivo* PC activity recordings from quiet wakefulness state to locomotive state, I measured the dilation of the pupil to measure the changing of behavioral state as well as LC activation, and motion of the forelimb of the animal by tracking limb motion using on-line analysis of the video sequence (Figure 2B). For *post-hoc* identification of the recording site and immunohistochemistry of zebrin modules, Hoechst 33345, which is a nucleic acid stain, was injected using a brief air-puff after successful recordings (Figure 3A). Z+/- PCs were later identified by staining aldolase C or zebrin II and grouped for analysis (Figure 3B).

PC SS output modulation during locomotion

PCs have been shown to operate at different firing frequencies depending on the expression of zebrin II during quiet wakefulness (Zhou et al., 2014). In line with the previous report, PC recordings from lobule V of the cerebellar vermis showed lower SS output in Z+ PCs (n = 12cells, 10 mice)

than in Z- PCs (n = 11 cells, 11 mice) during quiet wakefulness (Z+: 45.3 ± 6.19 Hz; Z-: 83 ± 10.98 Hz; two-sample t-test, ***p<0.001, Figure 4). CS also showed lower firing in Z+ modules than in Z- modules (Z+: 1.3 ± 0.09 Hz; Z-: 1.65 ± 0.15 Hz; two-sample t-test, *p<0.05; Figure 4).

To understand how these heterogeneously operated zebrin-dependent PCs act upon motor behavior, PCs from each module were recorded during quiet wakefulness and locomotion (Figure 5, 6). During the change in state from quiet wakefulness to locomotion, Z+ PCs significantly increased in SS frequency (Z+: n = 12 cells, quiet: 45.3 ± 6.34 Hz, locomotion: 81.1 ± 7.29 Hz; mean ± SEM, paired sample t-test; ***p<0.01), while SS activity of Z− PCs showed no significant difference in the change of state (Z−: n = 11 cells, quiet: 88.9 ± 13.7 Hz, locomotion: 96.8 ± 12.5 Hz; mean ± SEM, paired sample t-test; ns, non-significant; Figure 6A). Note that while the majority of the Z+ PCs increased in simple spike firing upon locomotion, Z− PCs had almost no response or decreased simple spike firing during locomotion. As for CS, PCs belonging to Z+ and Z− modules showed no difference in frequency during locomotion (Z+: quiet: 1.45 ± 0.08 Hz, locomotion: 1.48 ± 0.13 Hz; Z−: quiet: 1.74 ± 0.15 Hz, locomotion: 1.73 ± 0.14 Hz; mean ± SEM, paired sample t-test; ns, non-significant; Figure 6B). On contrary to Z− PCs, interspike intervals (ISI) of Z+ PC SSs showed a leftward shift in ISI during locomotion indicating an increase in burst firing (Figure 7). These results point towards that during locomotion, bidirectional firing which have been previously reported (Udo et al., 1981, Armstrong and Edgley, 1984, Armstrong and Edgley, 1988, Edgley

and Lidierth, 1988, Jelitai et al., 2016), are dependent on the expression of zebrin II.

NA-dependent modulation of PC SS output during locomotion

The LC projects axons to many brain regions including the cerebellum (Abbott and Sotelo, 2000, Sara, 2009). In addition, it has been reported that during locomotion, calcium transients in Bergmann glia of the cerebellum are induced by noradrenaline (Paukert et al., 2014). In order to examine the extent of the NA contribution on PC output, I administered a selective irreversible LC neurotoxin, N-(2-chloroethyl)-N-ethyl-2-bromobenzylamine (DSP-4) to mice via i.p. injection (Figure 8). DSP-4 destroys noradrenergic terminals thus nearly depleting the level of NA in the brain (Jonsson et al., 1981, Rommelfanger et al., 2007, Bekar et al., 2008, Ross and Stenfors, 2015). Interestingly, the enhancement of SS firing frequency during locomotion in Z+ PCs shown in non-treated controls were non-apparent in DSP-4 injected mice (n = 6 cells, 5 mice; quiet: 48.7 ± 5.45 Hz, locomotion: 75.4 ± 10.9 Hz, mean ± SEM, paired sample t-test, p = 0.12 ns; non-significant; Figure 8A, 9A). As for Z− PCs of DSP-4 treated mice, SS of Z− PCs did not respond during locomotion (n = 6 cells, 5 mice; quiet: 72.8 ± 13.5 Hz, locomotion: 77 ± 11.3 Hz, mean ± SEM, paired sample t-test, p = 0.77, ns; non-significant; Figure 9A). DSP-4 did not have effect on the CS firing rate in both zebrin modules in change of states (Z+: quiet: 1.23 ± 0.1 Hz, locomotion: 1.41 ± 0.23 Hz; Z−: quiet: 1.74 ± 0.07 Hz,

locomotion: 1.91 ± 0.11 Hz; mean ± SEM, paired sample t-test, ns; non-significant; Figure 9B). Thus, suggesting that during locomotion, only the SS of Z+ PC are modulated by NA.

DSP-4 disrupts forelimb trajectory during locomotion

In order to better understand the motion trajectory in which the Z+ PC SS output disrupted, I analyzed the trajectory of the forelimb by tracing the motion of the forepaw (Figure 10; See Materials and Methods). Although there were no differences in initiation of forward motion, while forelimb motion of non-treated control mice showed a stable repetitive motion, DSP-4 injected mice showed shorter range in stride motion (Control: stride motion: 21.5 ± 0.33 mm; DSP-4: stride motion: 16.9 ± 0.26 mm, mean ± SEM, two-sample t-test, ***$p<0.001$; Figure 10C). Stride velocity also showed difference between the two groups (Control: n = 3 mice, 9 trials, 18.4 ± 0.6 cm/s; DSP-4: n = 3, 18 trials, 14.8 ± 0.4 cm/s, mean ± SEM, two-sample t-test, ***$p < 0.001$; Figure 10D). No difference in stride frequency was shown (Figure 10E). Accordingly, the disruption of SS output modulation in Z+ PCs by NA depletion altered normal forelimb stride motion.

Local noradrenergic inhibition of cerebellar PC output

Given that the disruption in neuromodulation of PC SS output in Z+ modules in which altered normal limb motion was caused by DSP-4, a global effector, I investigated a more local and direct effect of NA on the cerebellum

by topical application of α_1, α_2, β_1, and β_2 adrenergic receptor antagonist cocktail (Cocktail; prazosin, yohimbine, betaxolol, and ICI 118,551, respectively) via the craniotomy window. Local infusion of drug and its time dependency were examined by local infusion of phenol red (Figure 11A). Intensity analysis shows 5 mins of topical application of the drug was diffused down to the PC layer which is 200 μm from the surface of the cerebellar cortex (Figure 11B). PC outputs were recorded for behavioral state changes under external solution application prior to drug application (Figure 12A). Identical PCs recorded for controls were maintained for the antagonist cocktail application (Figure 12B). Under the influence of the antagonist cocktail, the enhancement of SS frequency of Z+ PC (n= 4 cells, 4 mice) which was shown in control (Control: quiet: 48.1 ± 5.44 Hz, locomotion: 72.5 ± 4.61 Hz; mean ± SEM, paired sample t-test, *$p<0.05$, n = 4 cells, 4 mice; Figure 13A) were abolished during locomotion (Cocktail: quiet: 50.8 ± 7.67 Hz, locomotion: 54.8 ± 9.6 Hz; mean ± SEM; paired sample t-test, ns; non-significant; Figure 13B). However, no change was shown in CS frequency upon application (Control: quiet: 1.29 ± 0.29 Hz, locomotion: 1.18 ± 0.24 Hz; Cocktail: quiet: 1.45 ± 0.04 Hz, locomotion: 1.01 ± 0.34 Hz; mean ± SEM, paired sample t-test, ns; non-significant; Figure 13C, D). Z− PCs were also examined upon antagonist cocktail application (Figure 14). As in DSP-4 results, Z−PCs showed no change in SS firing frequency during behavioral state transition upon cocktail application (Z−: n = 4 cells, 4 mice; control: quiet: 51.8 ± 9.1 Hz, locomotion: 62.3 ± 16.6 Hz; Cocktail: quiet: 56 ± 10.7 Hz, locomotion: 71.6 ± 24.9 Hz;

mean ± SEM, paired sample t-test, ns; non-significant; Figure 15A, B). CS also showed no significant change upon cocktail application (Control: quiet: 1.2 ± 0.11 Hz, locomotion: 1.58 ± 0.32 Hz; Cocktail: quiet: 1.40 ± 0.16 Hz, locomotion: 1.66 ± 0.14 Hz; mean ± SEM, paired sample t-test, ns; non-significant; Figure 15C, D). In line with DSP-4 results, local inhibition of noradrenaline in vermal cortex of lobule V inhibits the increasing activity of SS in Z+ PCs during locomotion.

Normal forelimb motion upon cerebellar local NA inhibition

Despite the fact that cerebellar lobule V is well known for its contribution in limb coordination during locomotion (Ozden et al., 2012, Powell et al., 2015), unlike DSP-4, local inhibition of noradrenaline showed no effect in alteration in forelimb motion trajectory during locomotion (Figure 16A, B). Forelimb stride length showed no difference upon the application of local adrenergic receptor antagonists (Control: n = 6, 12 trials, stride: 17.3 ± 0.32 mm; Cocktail: n = 6, 18 trials, stride: 17.015 ± 0.3 mm, mean ± SEM, two-sample t-test, p = 0.51; Figure 16C). Stride velocity and frequency of stride under control and cocktail conditions showed no difference (Figure 16D).

α_2-AR effect on MLI firing during locomotion

Jelitai et al. (2016) has reported that bidirectional modulation of PCs occur due to the balance of excitatory-inhibitory input on to the PCs. However, what causes the difference in magnitude of MLI activity has yet not been

described. One of the possibilities of this difference in strength to occur is through the adrenergic receptors on the MLI. The α_1 and α_2-ARs have been identified immunohistochemically to exist on MLIs (Papay et al., 2006, Papay et al., 2004, Hirono et al., 2008). α_1 and α_2-ARs have been shown *in vitro* to dual modulate the activity of the MLIs upon activation which the concurred with IPSCs of PCs upon agonist application of each adrenergic receptor. While activation of α_1-ARs increases the activity of MLIs via Gq signaling pathway which activates phospholipase C thus increasing calcium which results in increase of activity, α_2-ARs activation decreases MLI firing thru the inhibition of voltage gated calcium channels, reduction of cAMP, and activation of inwardly rectifying K^+ channels resulting in decrease in activation (Hirono and Obata, 2006). In addition, behavior studies of α-AR knockout mice have shown that α_2-AR knockout show a more profound behavioral deficit in motor coordination and locomotion than in α_1-AR knockout mice(Lahdesmaki et al., 2002, Knauber and Muller, 2000, Mishima et al., 2004). Therefore, I examined the effect of α_2-AR antagonist, yohimbine (1mM), on MLI activity.

Inhibition of MLIs have been reported to be organized in parasagittal zones which aligns with zebrin II modules (Gao et al., 2006). I therefore distinguished the MLIs based on its location by *post-hoc* identification of the recording site. MLIs were identified by basal firing frequency, depth, and response to locomotion. MLIs were recorded during quiet wakefulness and locomotion state transition (Figure 17A, B and 18A, B). Identical cells recorded for control and yohimbine show that MLIs located in the Z+ and Z− modules increase in frequency during locomotion and there no significant change in

frequency upon application of yohimbine, 5 mins prior to recording (Z+: n = 3, Control: quiet: 14.8 ± 1.8 Hz, locomotion: 46.3 ± 8.8 Hz, p = 0.08; Yohimbine: quiet: 13.9 ± 5.5 Hz, locomotion: 46.4 ± 10.8 Hz, p = 0.08; Z−: n = 3, Control: quiet: 18.2 ± 6.5 Hz, locomotion:54 ± 24.8 Hz, p = 0.19; Yohimbine: quiet: 13.5 ± 4 Hz, locomotion: 51.4 ± 24.2 Hz, p = 0.2, mean ± SEM, paired sample t-test, Figure 17C, D and 18C, D). However, since MLIs in both modules increased in frequency during locomotion in control and α_2-AR blocked conditions, this cannot explain the discrepancy in magnitude of MLI activity which may show difference in SS activity between modules.

α_2-AR effect on Z+ PC SS activity

With the logic in mind that α_2-ARs are essential for motor coordination as seen in behavioral studies of α_2-AR knockout mice (Knauber and Muller, 2000, Lahdesmaki et al., 2002, Mishima et al., 2004), I tested whether α_2-ARs on PCs would effect SS firing in Z+ PCs during locomotion (Figure 19 and 20). SS of Z+ PCs which were enhanced during locomotion under control conditions, also showed an enhancement of SS activity under the influence of yohimbine (Figure 20A, B). CS of Z+ PCs which showed no change in frequency during locomotion under control conditions, also showed no changes in firing frequency with the effect of the α_2-AR antagonist (Figure 20). Although more recordings are needed to conclude this observation, but showing that the results are consistant in the recorded Z+ PCs, it is safe to say that α_2-ARs on PCs does not effect the SS output of Z+ PCs.

Inhibition of β_2-ARs suppress enhancement of PC SS in Z+ modules

β-ARs have been shown to be expressed and function in the cerebellum (Saitow et al., 2005, Lippiello et al., 2015). Among the two subtypes of β-ARs, β_2-ARs are most abundantly expressed in PC dendrites, PC layer, and granule cell layers (Lippiello et al., 2015). β-ARs have been shown to activate cAMP and PKA signaling via activation of Gs protein (Skalhegg and Tasken, 2000, Taylor et al., 2012), which ultimately enahnces signaling in synapses. Lippiello et al. (2015) have shown that activation of β-ARs,especially β_2-ARs, at PF-PC sysnapse, enhances in which activated β-ARs lowers the threshold for potentiation. Thus, I hypothesized that the enhancement of SS activity shown in Z+ PCs may be due to the effect of β_2-ARs on PCs which would lower the threshold to enhance activity thus giving a robust SS enhancement during locomotion.

Accordingly, I examined the effect of β_2-ARs on Z+ PCs during locomotion by topically applying ICI 118,551 (1 mM), a selective β_2-AR antagonist (Figure 21 and 22). During locomotion, activity of Z+ PC SS enhance (Figure 21A and 22A). However, upon 5 minutes of topical application of ICI 118,551, the enhancement is suppressed and does not enhance significantly as much as it did in control conditions (n = 3, Control: quiet: 40.3 ± 11.7 Hz, locomotion: 83.9 ± 22.2 Hz, mean ± SEM, paired sample t-test, p =0.07; ICI 118,551: quiet: 43.5 ± 13.6 Hz, locomotion: 71.8 ± 20 Hz, mean ± SEM, paired sample t-test, p = 0.18; Figure 21B and 22B). CS activity did not

change under the influence of the β_2-AR blocker (n = 3, Control: quiet: 1.38 ± 0.29 Hz, locomotion: 1.15 ± 0.18 Hz, p = 0.1 ; ICI 118, 551: quiet: 1.4 ± 0.26 Hz, locomotion: 1.31 ± 0.48 Hz; mean ± SEM, paired sample t-test, p = 0.78; Figure 22C, C).

A

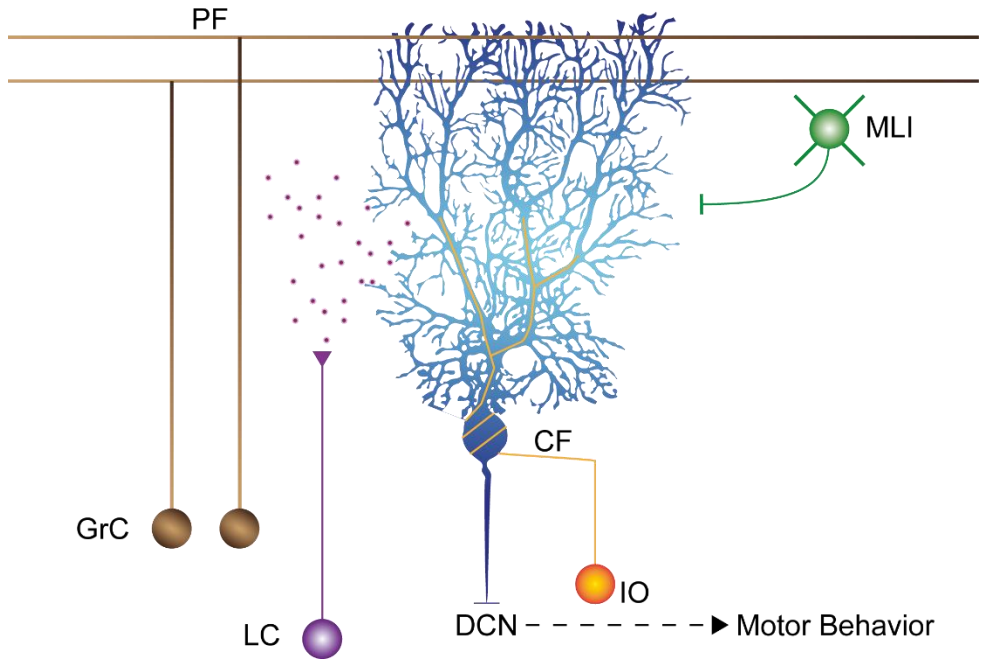
PF
MLI
CF
GrC
IO
LC
DCN
Motor Behavior

B

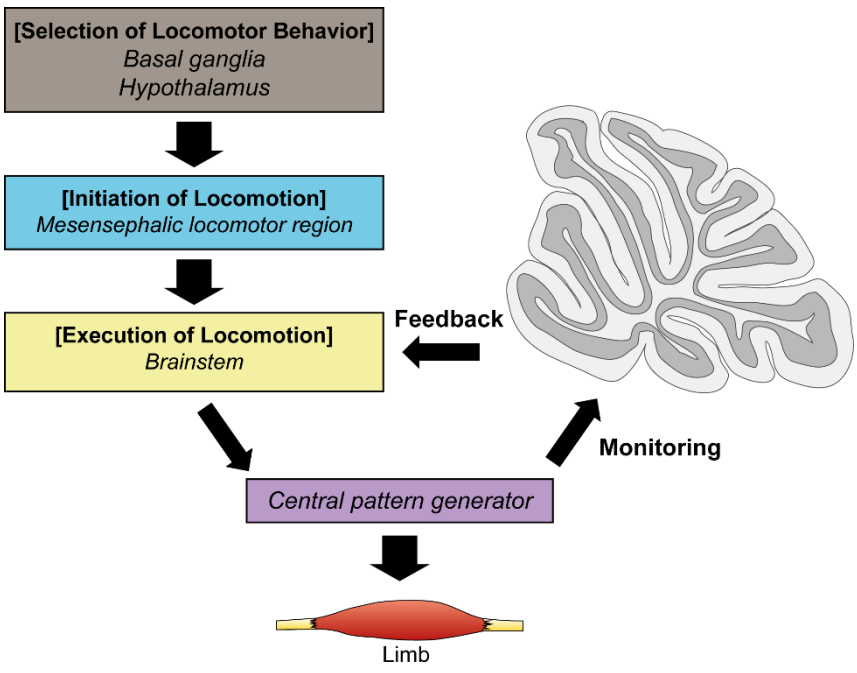
[Selection of Locomotor Behavior]
Basal ganglia
Hypothalamus
[Initiation of Locomotion]
Mesensephalic locomotor region
[Execution of Locomotion]
Brainstem
Feedback
Monitoring
Central pattern generator
Limb

Figure 1. The involvement of the cerebellum in the control of locomotion behavior

(A) Diagram of brain circuits underlying locomotion behavior. Selection of locomotion is executed in the basal ganglia and hypothalamus. Locomotion is initiated in the mesencephalic locomotor region which projects the brainstem to execute behavior. This information is conveyed to the central pattern generator of the spinal cord to generate a rhythmic pattern of activity to motor neurons to activate muscle movement for locomotion. The cerebellum coordinates motor behavior by monitoring the sensory feedback, as well as the patterns generated by the central pattern generator, and modulating the activity of the brainstem to adjust to changes in the environment. (B) Cerebellar circuit involved in locomotion behavior. Monitored inputs are sent via the mossy fibers which project to activate the granule cells (GrC). The Purkinje cell (PC) receives inputs from parallel fibers (PF), which are GrC axons, inputs from the inferior olive (IO) through the climbing fiber (CF), and noradrenergic inputs from the locus coeruleus (LC) projecting its output to the deep cerebellar nucleus (DCN). The DCN projects to the brainstem, spinal cord, and motor neurons to execute motor behavior.

A

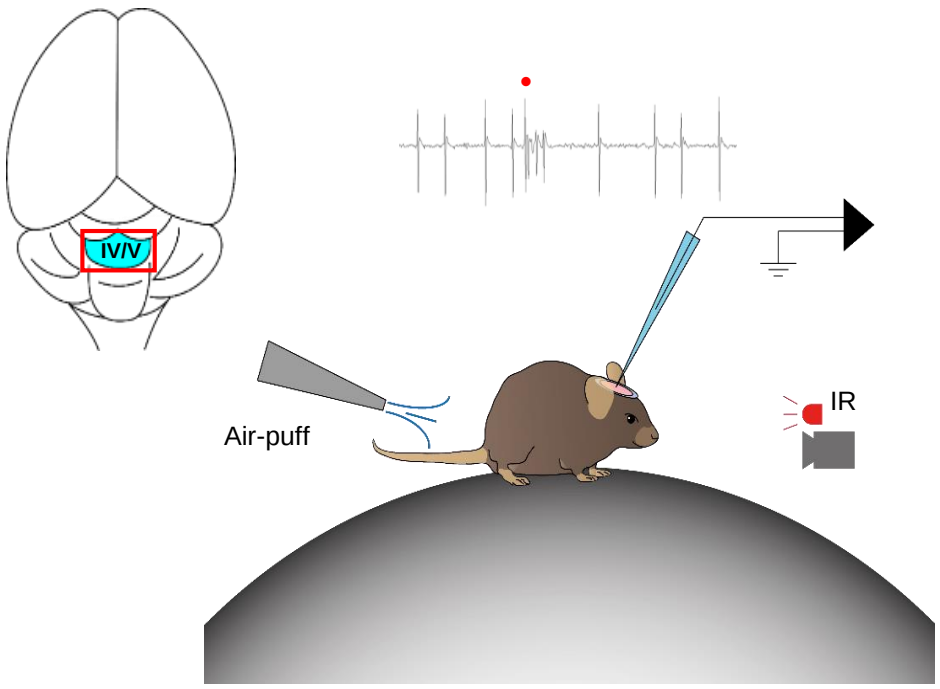

B

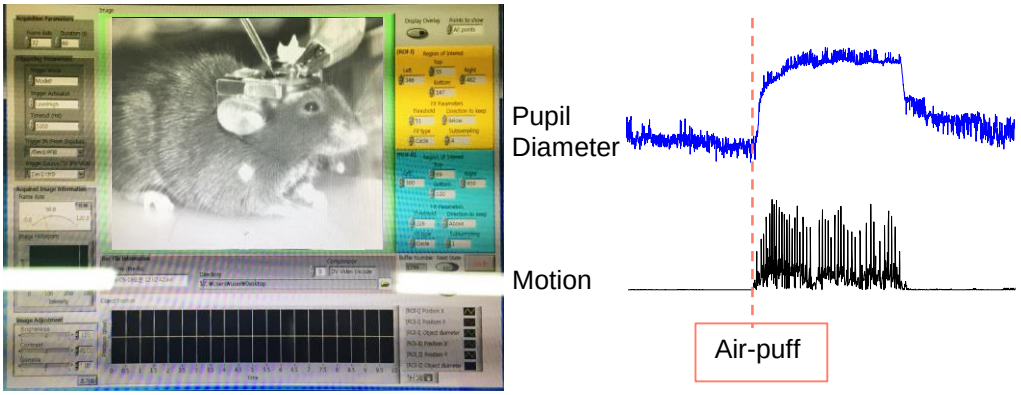

Figure 2. *In vivo* PC recording configuration and motion tracking in awake mice

(A) Recording location (cerebellar lobule IV/V) and configuration in awake behaving mice on a cylindrical treadmill. Motion capture using digital camera and infrared (IR) light. (B) Custom made LabVIEW software for motion tracking. Motion tracking of IR reflective paint marked on the right forepaw was done during time of electrophysiological recordings. Pupil diameter and limb motion was analyzed on-line.

A

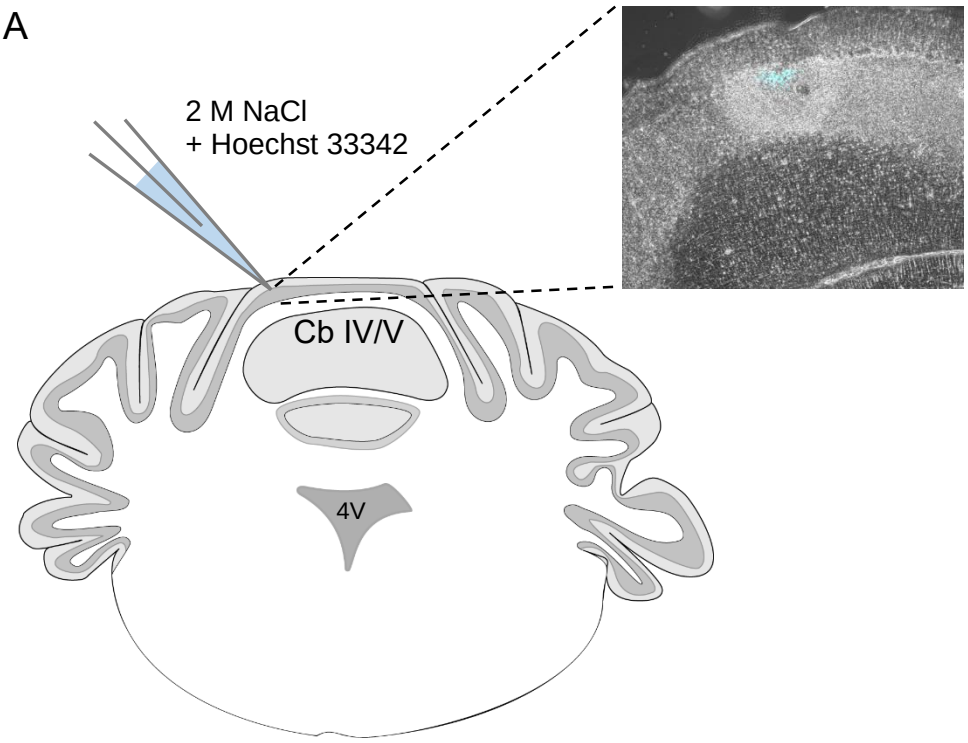

B

Zebrin + PC

Zebrin - PC

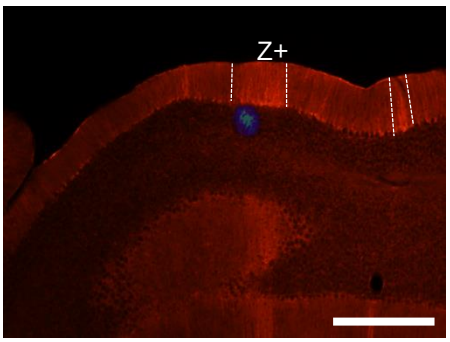

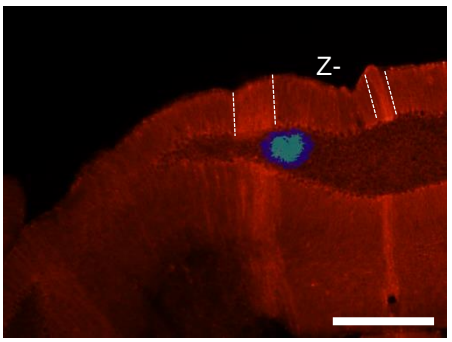

Figure 3. *Post-hoc* identification of recorded PC site and Aldolase C/ Zebrin II

(A) After successful recording, Hoechst 33342 was injected by brief air-puff to locate recording site *post-hoc*. (B) *Post-hoc* immunohistochemistry was done for aldolase C/ zebrin II in every successful recording. Data was sorted after immunohistochemical analysis of zebrin II and recording site. Scale bars indicate 300 μm.

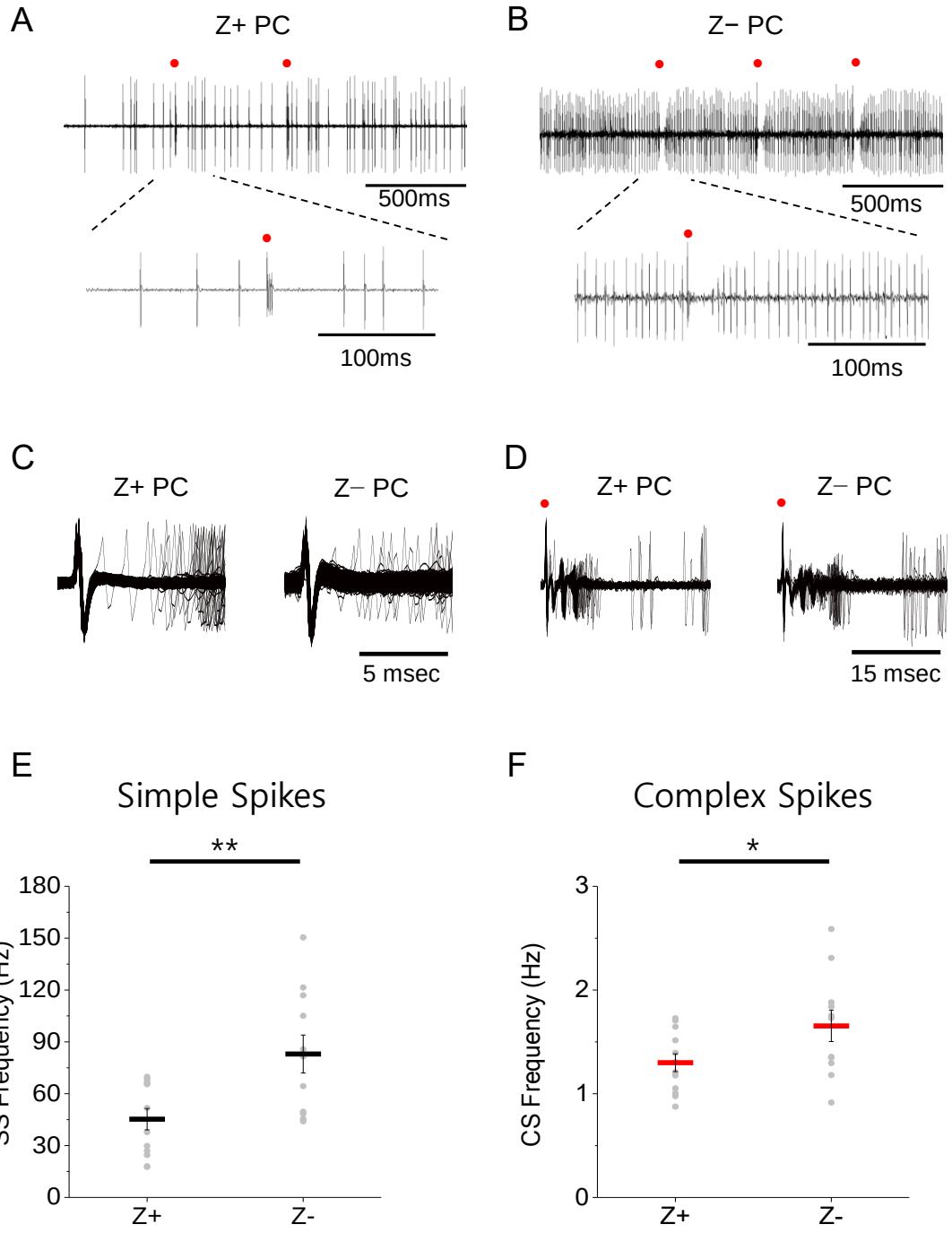
A
Z+ PC
500ms
100ms
B
Z− PC
500ms
100ms
C
Z+ PC
Z− PC
5 msec
D
Z+ PC
Z− PC
15 msec
E
Simple Spikes
**
SS Frequency (Hz)
180
150
120
90
60
30
0
Z+
Z-
F
Complex Spikes
*
CS Frequency (Hz)
3
2
1
0
Z+
Z-

Figure 4. Zebrin-dependent SS and CS activity during quiet wakefulness state in awake mice

Representative raw trace of (A) zebrin-positive (Z+) and (B) zebrin-negative (Z−) PCs. Red dots indicate complex spikes. (C, D) Overlay of simple and complex spikes of a single neuron from each module. Recordings were confirmed as single neuron recordings by simple spike and complex spike shapes. (E) Distribution of simple spike frequency (left) in Z+ and Z− PCs (mean ± SEM; black). Simple spike firing frequency is significantly lower in Z+ PCs in comparison to Z− PCs (Z+: 45.3 ± 6.19 Hz, n = 12 cells, 10 mice; Z−: 83 ± 11 Hz, n = 11 cells, 11 mice; two-sample t-test, ***$p<0.001$). Distribution of complex spike frequency (right) in Z+ and Z− PCs (mean ± SEM; red). Baseline complex spike firing frequency in Z+ PCs are lower compared to Z- PCs (Z+: 1.3 ± 0.09 Hz; Z−: 1.65 ± 0.15 Hz; two-sample t-test, *$p<0.05$).

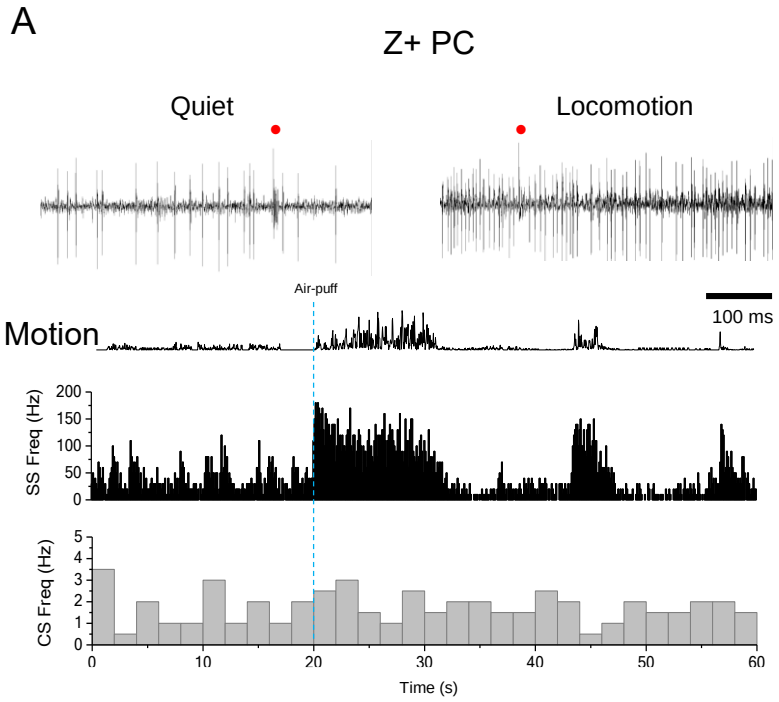
A
Z+ PC
Quiet
Locomotion
Air-puff
100 ms
Motion
SS Freq (Hz)
200
150
100
50
0
CS Freq (Hz)
5
4
3
2
1
0
0
10
20
30
40
50
60
Time (s)

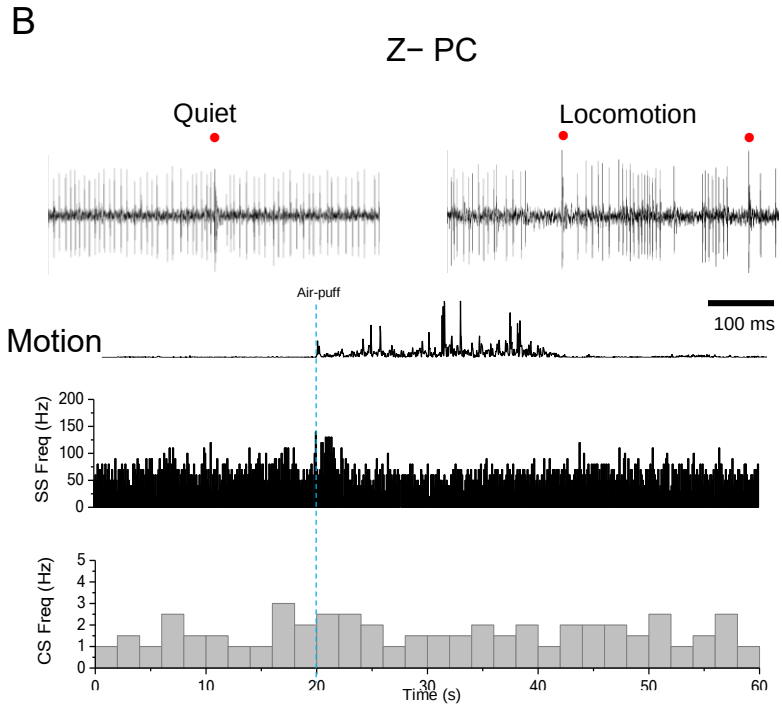
B
Z− PC
Quiet
Locomotion
Air-puff
100 ms
Motion
SS Freq (Hz)
200
150
100
50
0
CS Freq (Hz)
5
4
3
2
1
0
0
10
20
30
40
50
60
Time (s)

Figure 5. Behavioral state-dependent differential activity of PCs

(A, B) Representative single-unit electrophysiological traces from Z+ and Z- PCs which displayed enhanced activity and no response during locomotion, respectively. Motion detection during quiet and locomotion after air-puff. Peri-stimulus time histogram of simple spike (black; upper bottom) and complex spike (grey; lower bottom) during change in behavioral state (quiet and locomotion).

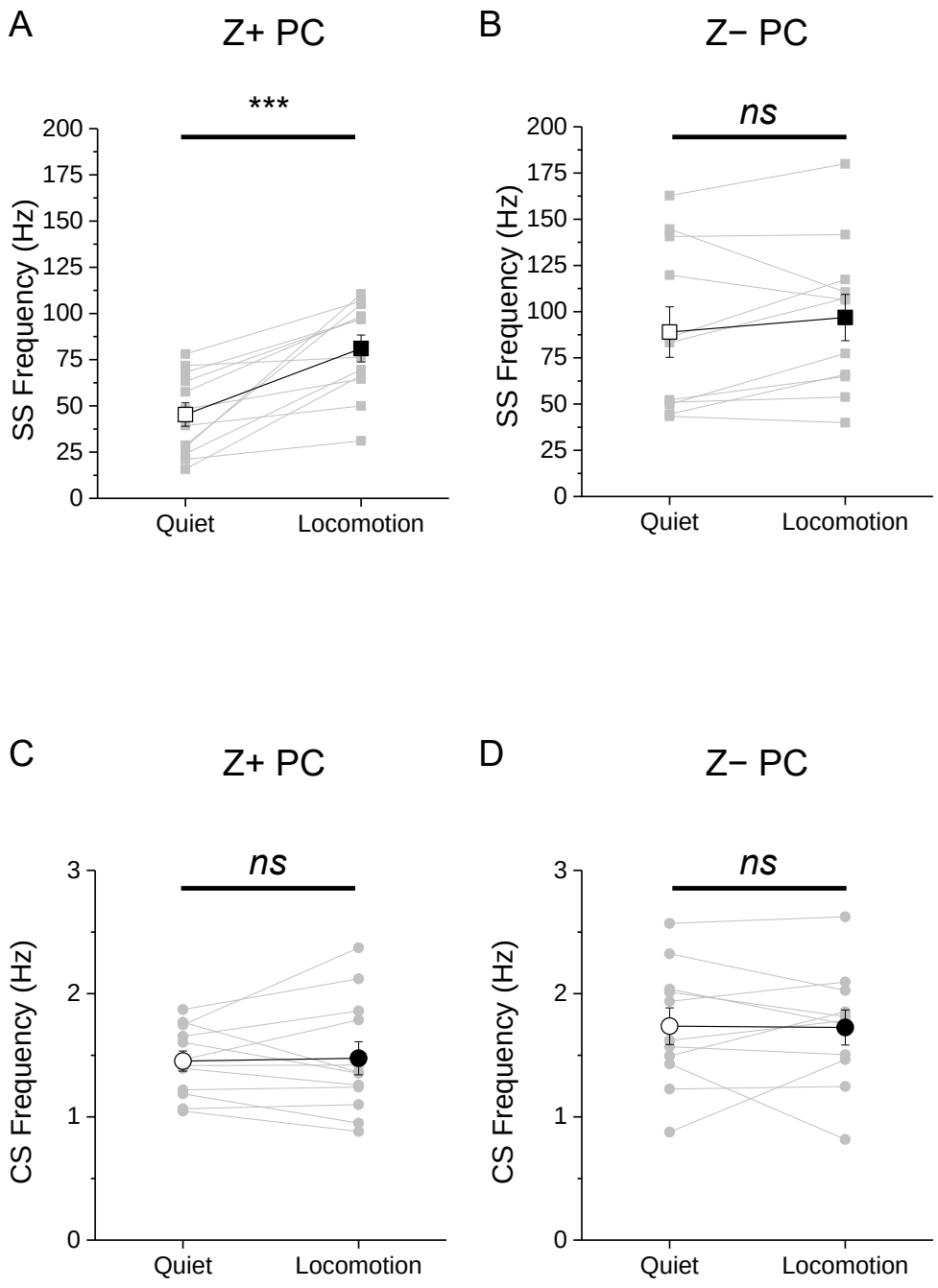
A
Z+ PC
***
SS Frequency (Hz)
200
175
150
125
100
75
50
25
0
Quiet
Locomotion
B
Z− PC
ns
SS Frequency (Hz)
200
175
150
125
100
75
50
25
0
Quiet
Locomotion
C
Z+ PC
ns
CS Frequency (Hz)
3
2
1
0
Quiet
Locomotion
D
Z− PC
ns
CS Frequency (Hz)
3
2
1
0
Quiet
Locomotion

Figure 6. Increased simple spike activity of Z+ PCs during locomotion

(A) Individual cell firing frequency distribution (filled grey circles) and mean of simple spike frequency during quiet wakefulness (black filled square) and locomotion (blue filled square) in Z+ PCs and Z- PCs. Z+ PCs showed a significant increase in simple spike activity during locomotion (Z+: n = 12 cells, quiet: 45.3 ± 6.34 Hz, locomotion: 81.1 ± 7.29 Hz; mean ± SEM, paired sample t-test; ***$p<0.01$) while Z- PCs had no significant change in simple spike firing frequency (Z-: n = 11 cells, quiet: 88.9 ± 13.7 Hz, locomotion: 96.8 ± 12.5 Hz; mean ± SEM, paired sample t-test; ns, non-significant). (B) Individual cell firing frequency distribution (open grey circles) and mean of complex spike frequency during state transition from quiet wakefulness (open black square) to locomotion (open blue square). Z+ PCs and Z- PCs showed no significant change in complex spike firing frequency during locomotion (Z+: quiet: 1.45 ± 0.08 Hz, locomotion: 1.48 ± 0.13 Hz; Z-: quiet: 1.74 ± 0.15 Hz, locomotion: 1.73 ± 0.14 Hz; mean ± SEM, paired sample t-test; ns, non-significant).

A

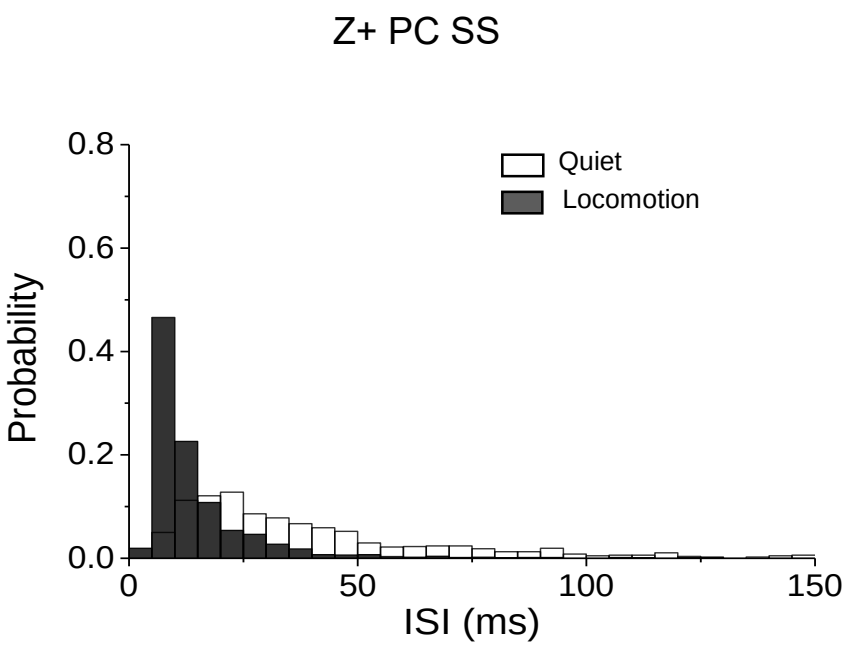
Z+ PC SS
Quiet
Locomotion
Probability
0.0
0.2
0.4
0.6
0.8
0
50
100
150
ISI (ms)

B

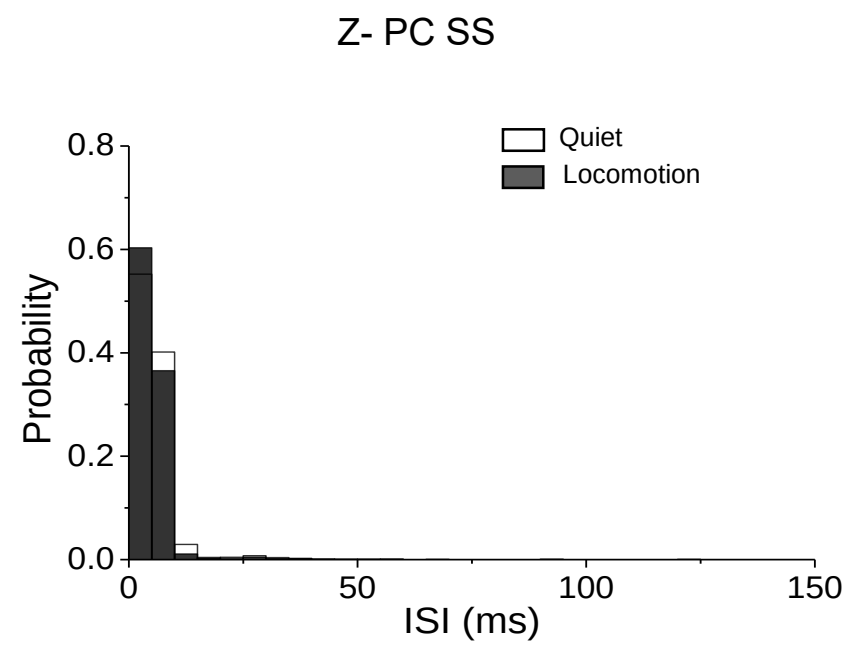
Z- PC SS
Quiet
Locomotion
Probability
0.0
0.2
0.4
0.6
0.8
0
50
100
150
ISI (ms)

Figure 7. Change in simple spike firing patterns during locomotion in Z+ PC

Simple spike inter-spike interval (ISI) distribution during quiet wakefulness (white) and locomotion (dark grey). (A) Z+ PC simple spike interspike intervals shifted to the left showing increase of burst firing during locomotion. (B) Z- PC showed no change in simple spike firing pattern.

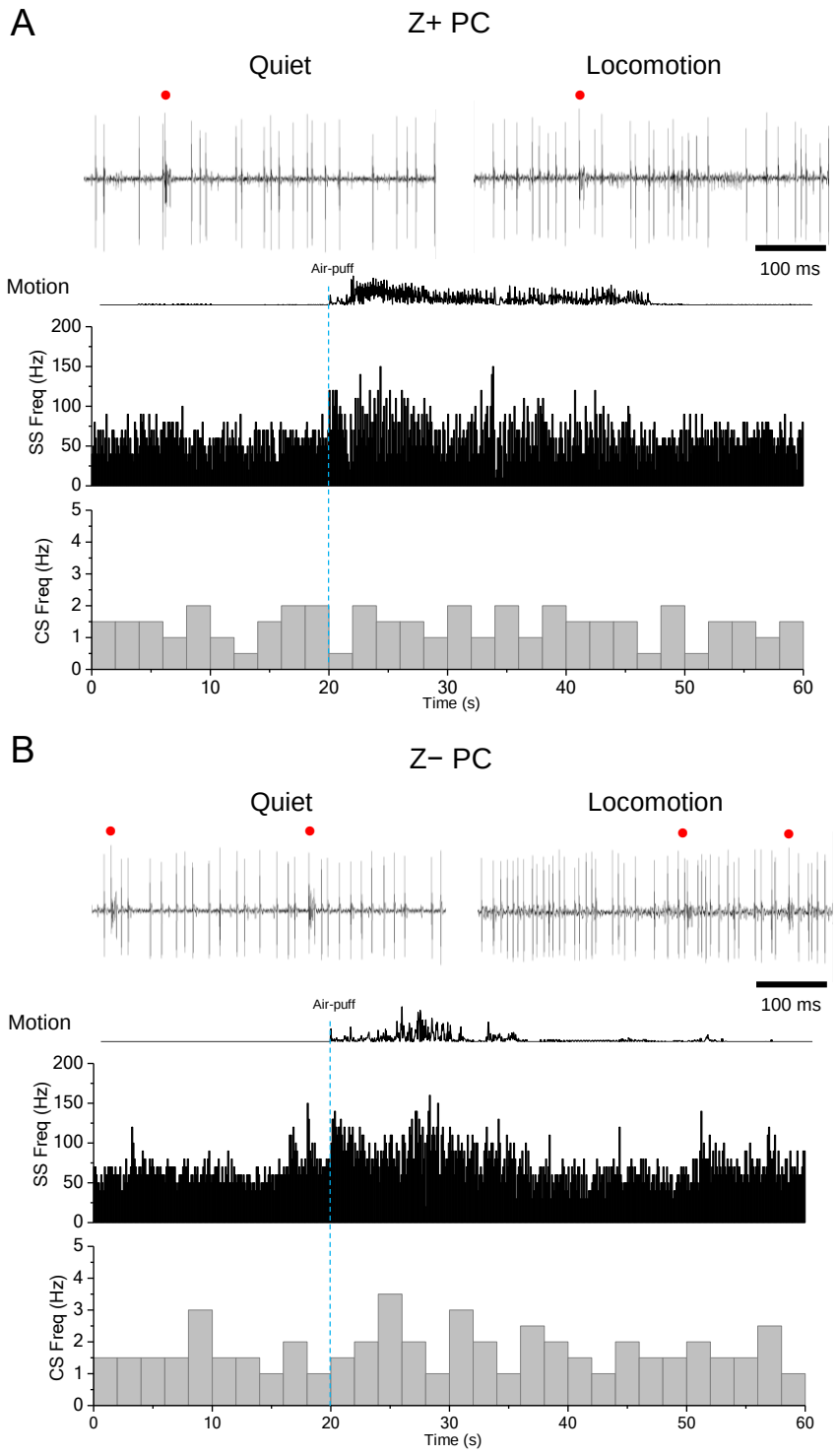
A
Z+ PC
Quiet
Locomotion
100 ms
Air-puff
Motion
SS Freq (Hz)
CS Freq (Hz)
Time (s)
B
Z− PC
Quiet
Locomotion
100 ms
Air-puff
Motion
SS Freq (Hz)
CS Freq (Hz)
Time (s)

Figure 8. Z+ and Z− PC firing activity upon reduction of noradrenergic input via DSP-4

Representative trace of PC activity in each zebrin module 7 days post-injection of DSP-4 (i.p. administration). Raw trace during quiet wakefulness and locomotion after air-puff in (A) Z+ and (B) Z− PCs. Asterisks indicate complex spikes. Peri-stimulus time histogram of simple spike (black) and complex spike (grey) show change of firing activity during quiet and locomotion under the influence of DSP-4.

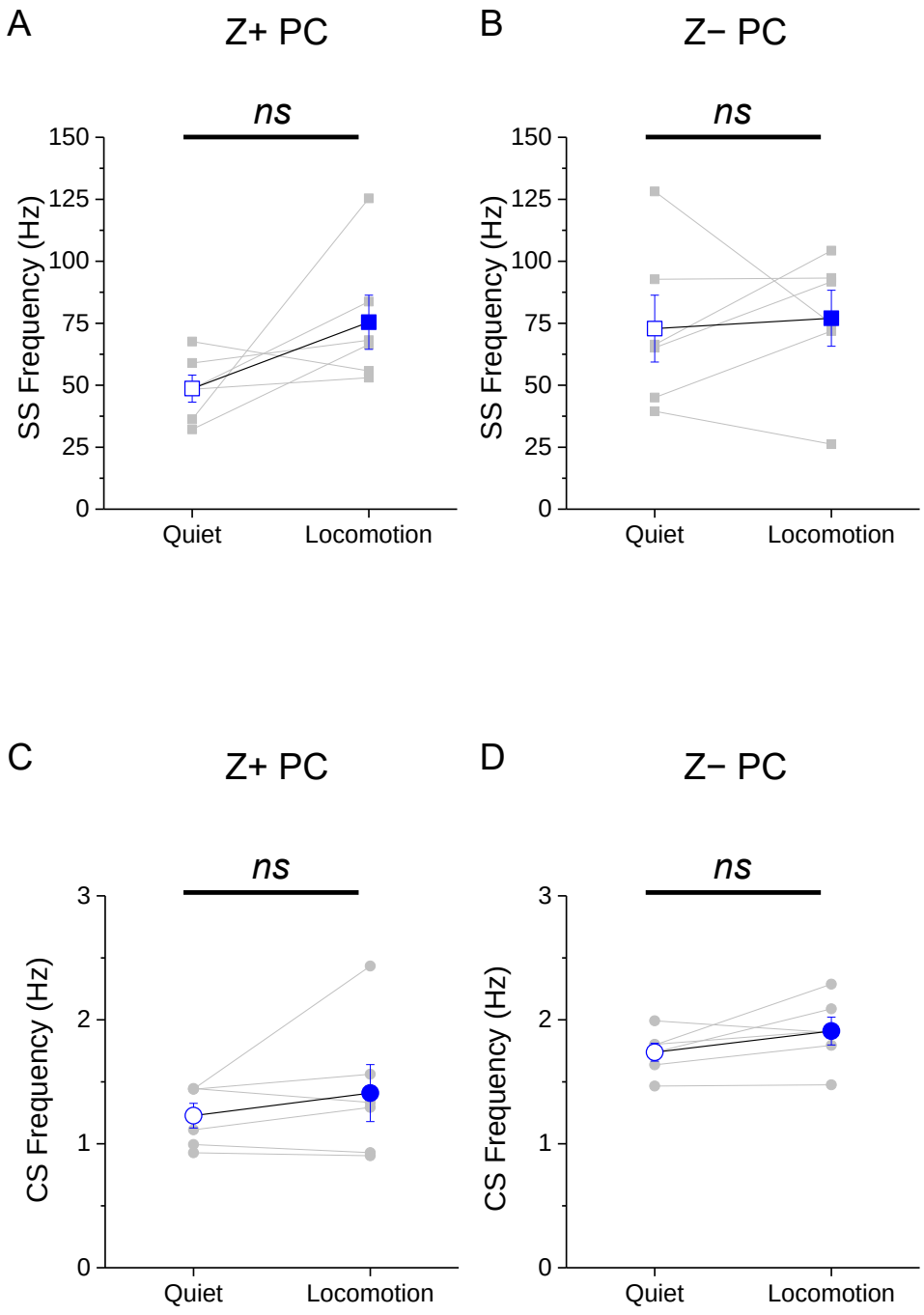
A
Z+ PC
ns
SS Frequency (Hz)
150
125
100
75
50
25
0
Quiet
Locomotion
B
Z− PC
ns
SS Frequency (Hz)
150
125
100
75
50
25
0
Quiet
Locomotion
C
Z+ PC
ns
CS Frequency (Hz)
3
2
1
0
Quiet
Locomotion
D
Z− PC
ns
CS Frequency (Hz)
3
2
1
0
Quiet
Locomotion

Figure 9. DSP-4 disrupts noradrenergic simple spike modulation of Z+ PC activity during locomotion

(A) Simple spikes firing frequency mean and individual cells during quiet wakefulness and air-puff induced locomotion. The increase of simple spikes during locomotion shown in Z+ PCs was disrupted in DSP-4 injected mice (n = 6 cells, 5 mice; quiet: 48.7 ± 5.45 Hz, locomotion: 75.4 ± 10.9 Hz, mean ± SEM, paired sample t-test, ns; non-significant). (B) Z- PCs show nearly no response or decrease of simple spike activity during locomotion showing no change under the influence of DSP-4 (n = 6 cells, 5 mice; quiet: 72.8 ± 13.5 Hz, locomotion: 77 ± 11.3 Hz, mean ± SEM, paired sample t-test, ns; non-significant). (C, D) Change in complex spike frequency during locomotion was not shown in neither modules (Z+: quiet: 1.23 ± 0.1 Hz, locomotion: 1.41 ± 0.23 Hz; Z-: quiet: 1.74 ± 0.07 Hz, locomotion: 1.91 ± 0.11 Hz; mean ± SEM, paired sample t-test, ns; non-significant).

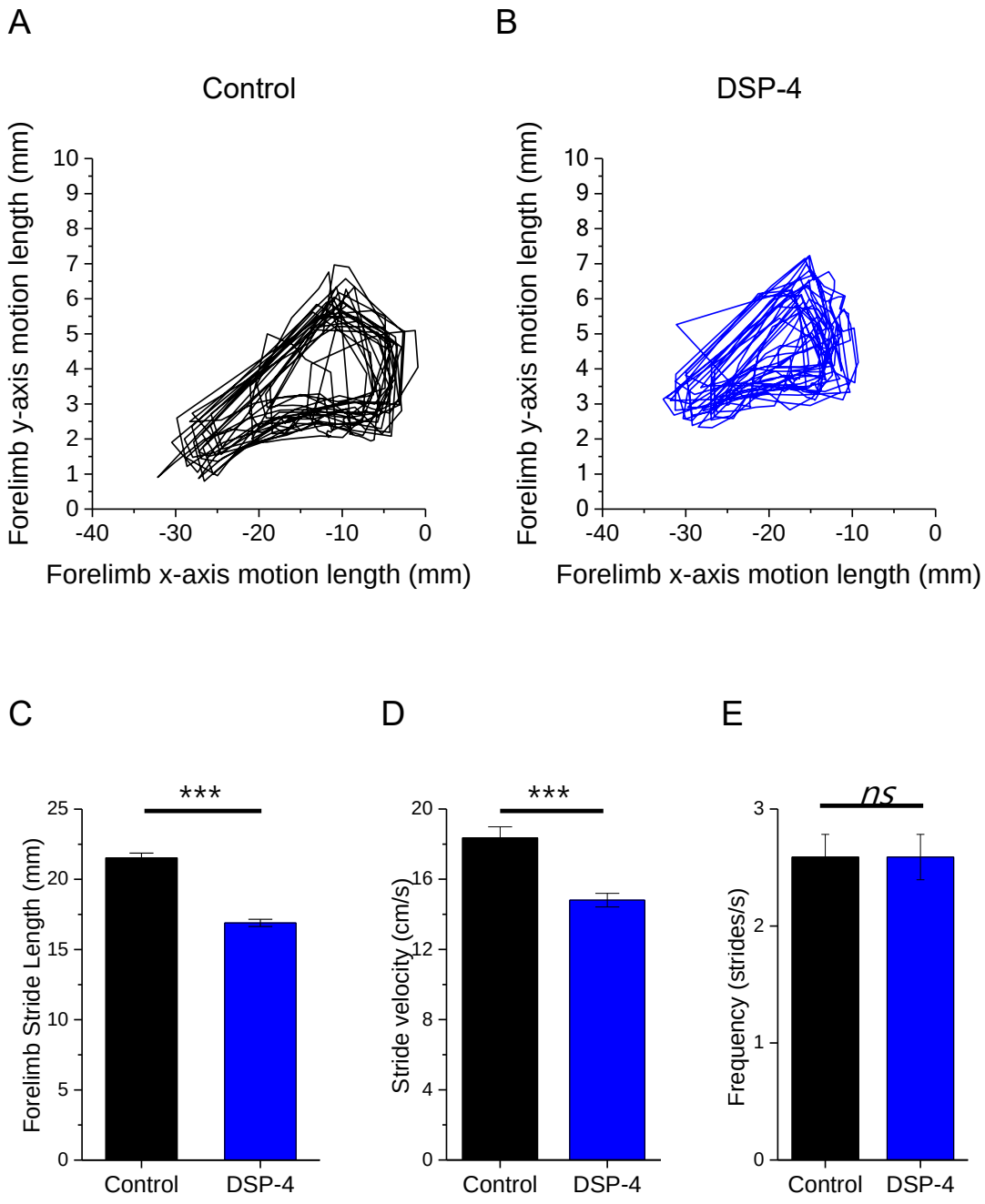
A
Control
Forelimb y-axis motion length (mm)
Forelimb x-axis motion length (mm)
B
DSP-4
Forelimb y-axis motion length (mm)
Forelimb x-axis motion length (mm)
C
***
Forelimb Stride Length (mm)
Control
DSP-4
D
***
Stride velocity (cm/s)
Control
DSP-4
E
ns
Frequency (strides/s)
Control
DSP-4

Figure 10. Abnormal limb motion in DSP-4 injected mice

(A) Representative trajectory of forelimb motion trajectory of control mouse. (B) Representative trajectory of forelimb motion trajectory of DSP-4 injected mouse (7 days post-injection). (C) Stride of DSP-4 injected mice are significantly shorter in length than that of control mice (Control: n = 3 mice, 21.9 ± 0.3 mm; DSP-4: n = 3 mice, , 16.2 ± 0.2 mm, mean ± SEM, two-sample t-test, ***p < 0.001). (D) Velocity of each stride during locomotion. (Control: n = 3 mice, 9 trials, 18.4 ± 0.6 cm/s; DSP-4: n = 3, 18 trials, 14.8 ± 0.4 cm/s, mean ± SEM, two-sample t-test, ***p < 0.001). (E) Frequency of limb motion during locomotion measured in control and DSP-4 mice (Control: 2.6 ± 0.2 strides/s; DSP-4: 2.8 ± 0.1, mean ± SEM, two-sample t-test, ns; non-significant).

A

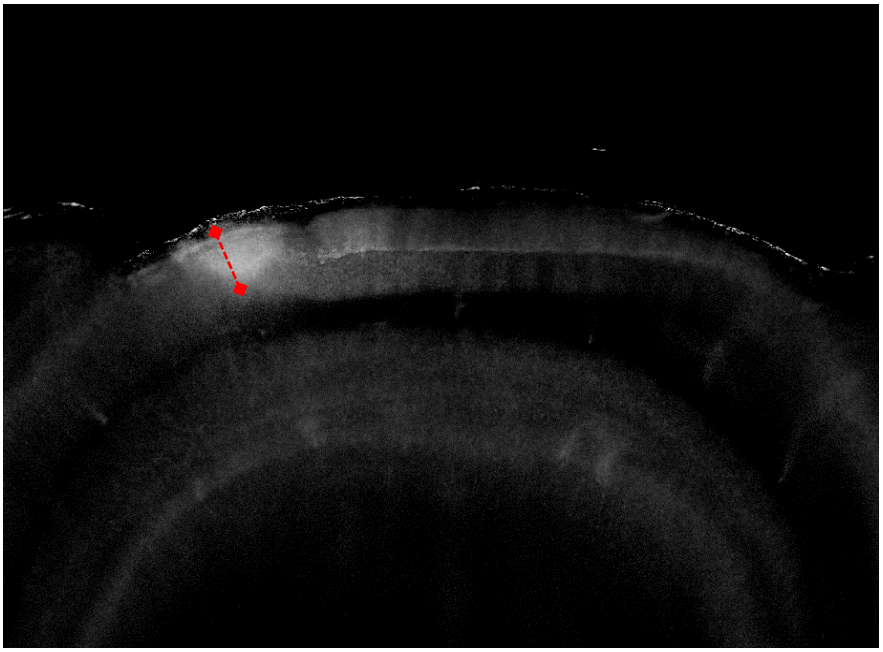

B

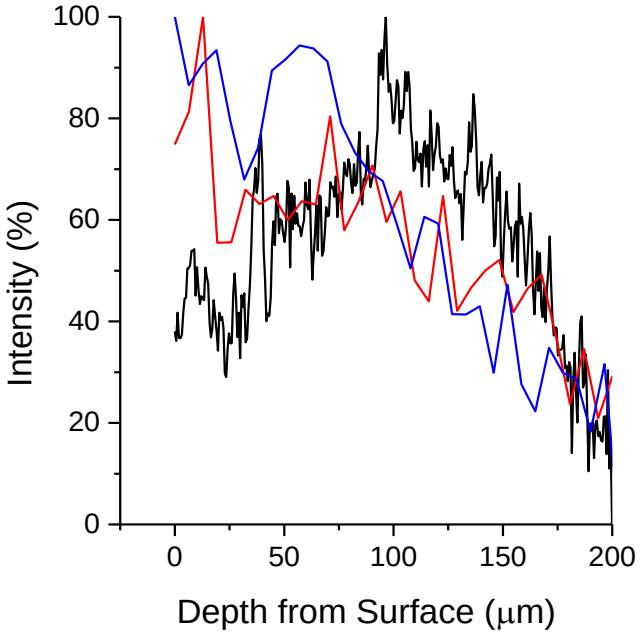
100
80
60
40
20
0
Intensity (%)
0
50
100
150
200
Depth from Surface (μm)

Figure 11. Drug diffusion through the cerebellar cortex

(A) Inverted image of phenol red (10 mM) dye diffusion through the cerebellar cortex after 5 min of topical application via the cranial window. (B) Dye intensity was measured in relation to depth from surface (Red dashed line in panel A).

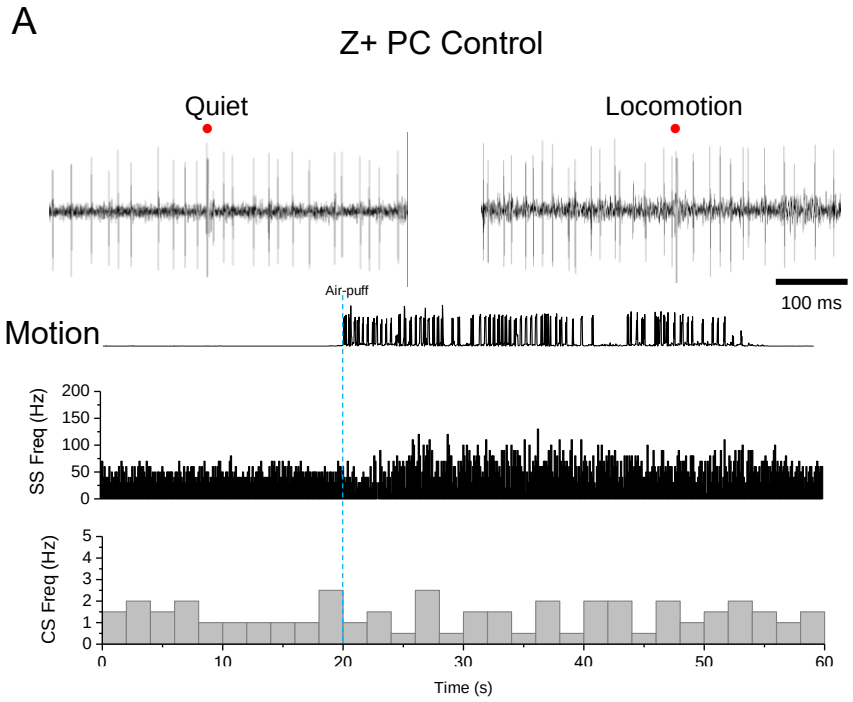
A
Z+ PC Control
Quiet
Locomotion
100 ms
Air-puff
Motion
SS Freq (Hz)
CS Freq (Hz)
Time (s)

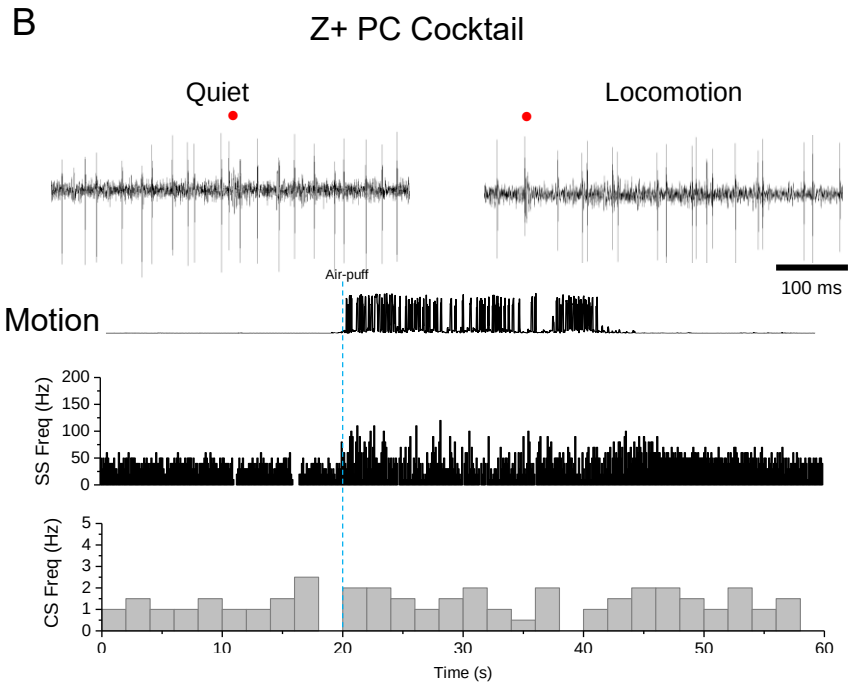
B
Z+ PC Cocktail
Quiet
Locomotion
100 ms
Air-puff
Motion
SS Freq (Hz)
CS Freq (Hz)
Time (s)

Figure 12. The effect of local and direct inhibition of adrenergic receptors on Z+ PC activity

(A) Representation of simple (black) and complex (grey) spike activity of a Z+ PC in control condition during quiet wakefulness and locomotion shown in peri-stimulus time histogram. (B) Recording of an identical cell as in (A), 5 mins after adrenergic receptor antagonist cocktail (Cocktail) application. Peri-stimulus time histogram of simple spike (black) and complex spike (grey) firing during quiet and locomotion behavioral states.

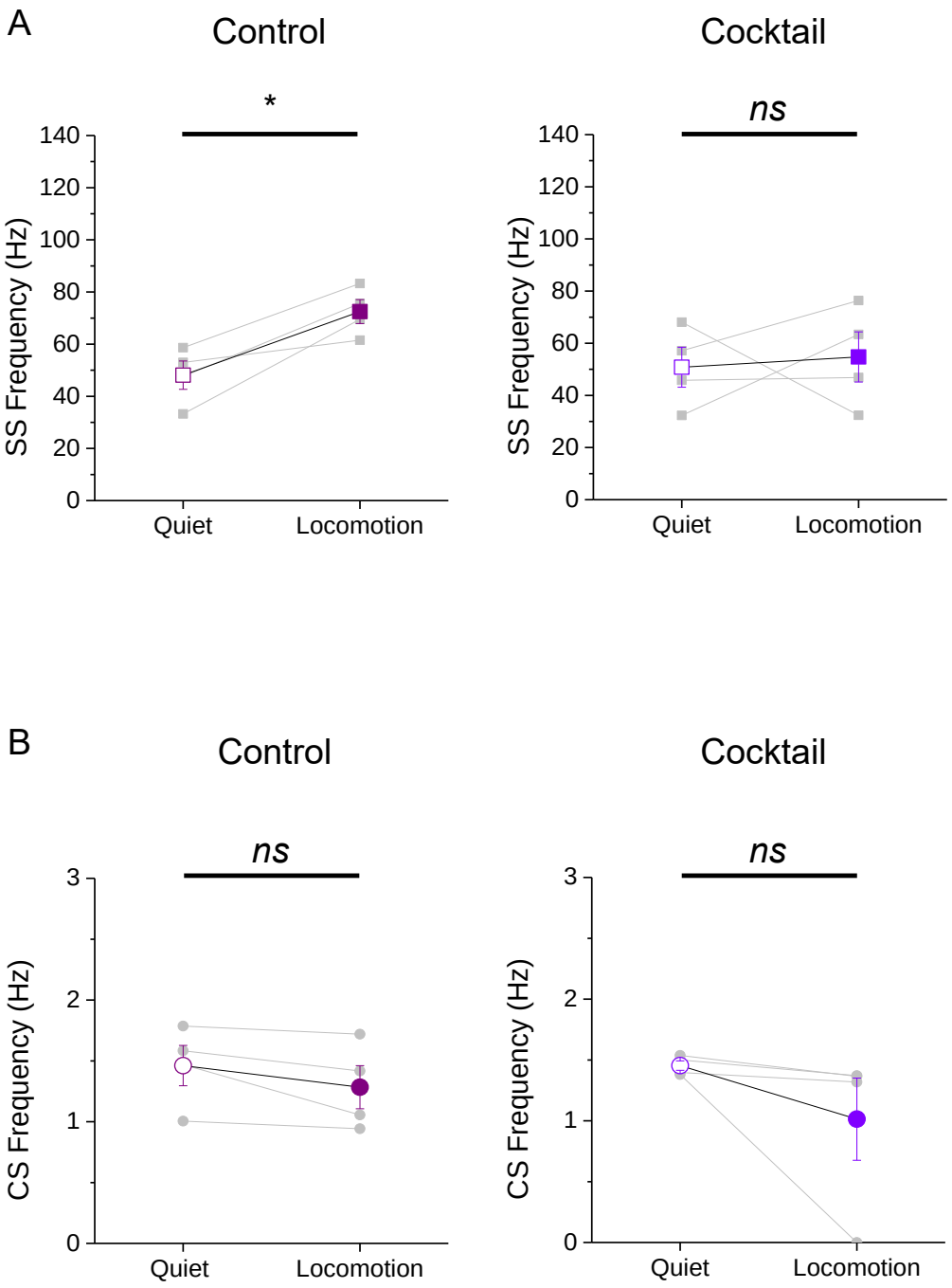
A
Control
Cocktail
*
ns
SS Frequency (Hz)
0
20
40
60
80
100
120
140
Quiet
Locomotion
B
Control
Cocktail
ns
ns
CS Frequency (Hz)
0
1
2
3
Quiet
Locomotion

Figure 13. Local inhibition of noradrenaline input by adrenergic receptor antagonist cocktail reduces enhancement of Z+ PC simple spike activity

(A) Enhancement in simple spike frequency of Z+ PC in control was abolished after 5 min topical application of adrenergic receptor antagonist cocktail (Control: quiet: 48.1 ± 5.44 Hz, locomotion: 72.5 ± 4.61 Hz; Cocktail: quiet: 50.8 ± 7.67 Hz, locomotion: 54.8 ± 9.6 Hz; mean ± SEM, paired sample t-test, *$p<0.05$, ns; non-significant, n = 4 cells, 4 mice). (B) Complex spikes showed no difference before or after application of adrenergic receptor antagonist cocktail during behavioral transition (Control: quiet: 1.29 ± 0.29 Hz, locomotion: 1.18 ± 0.24 Hz; Cocktail: quiet: 1.45 ± 0.04 Hz, locomotion: 1.01 ± 0.34 Hz; mean ± SEM, paired sample t-test, ns; non-significant). Recordings of topical application of external solution (control) or adrenergic receptor antagonist cocktail were done in the same cell.

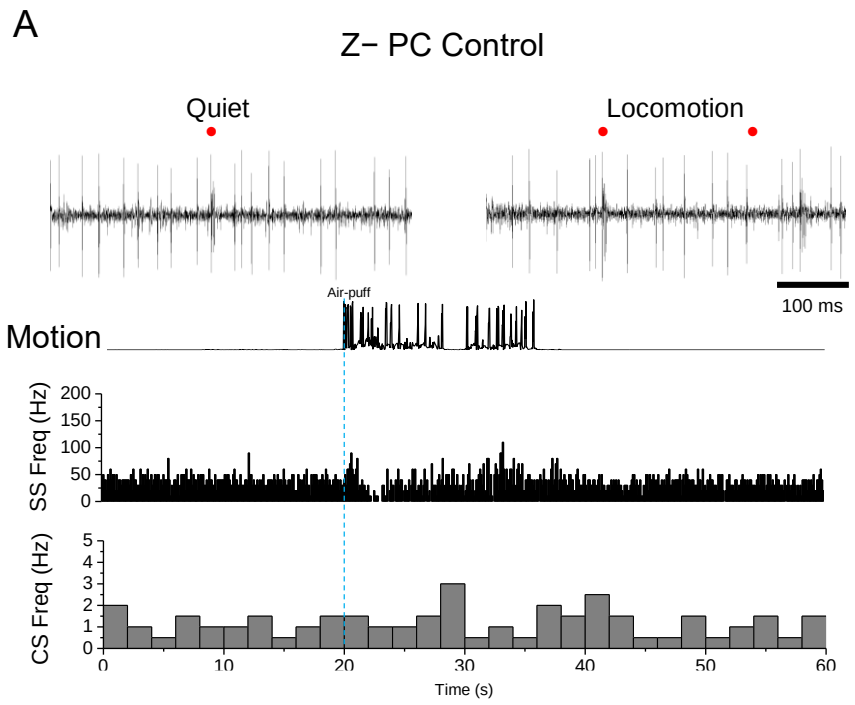
A
Z− PC Control
Quiet
Locomotion
100 ms
Air-puff
Motion
SS Freq (Hz)
CS Freq (Hz)
Time (s)

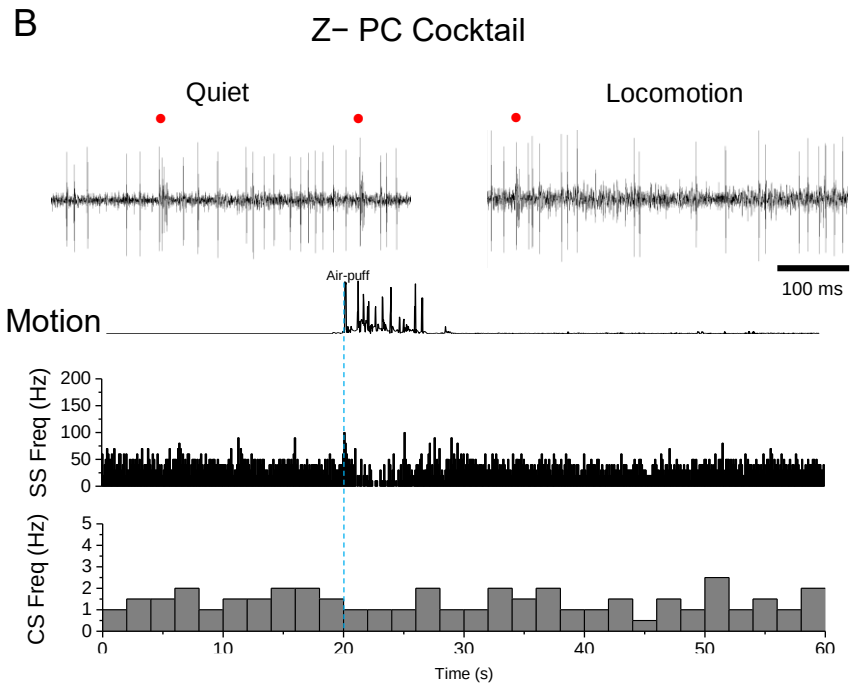
B
Z− PC Cocktail
Quiet
Locomotion
100 ms
Air-puff
Motion
SS Freq (Hz)
CS Freq (Hz)
Time (s)

Figure 14. The effect of local and direct inhibition of adrenergic receptors on Z− PC activity

(A) Representation of Z− PC in control condition simple (black) and complex (grey) spike activity during quiet wakefulness and locomotion shown in peri-stimulus time histogram. (B) Simple and complex spike activity 5 mins after adrenergic receptor antagonist cocktail (Cocktail) application. Peri-stimulus time histogram of simple spike (black) and complex spike (grey) firing during quiet and locomotion behavioral states.

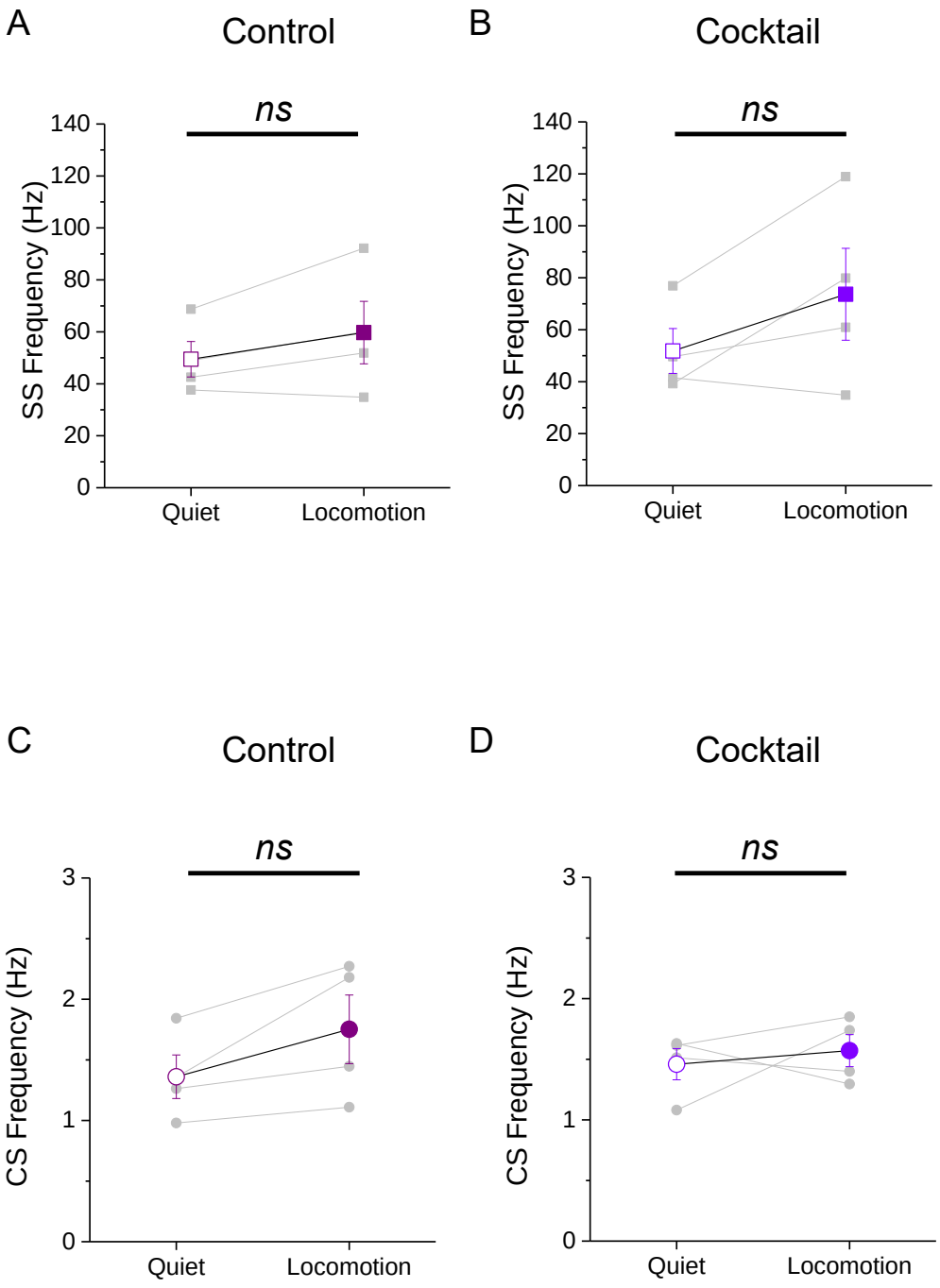
A
Control
ns
SS Frequency (Hz)
140
120
100
80
60
40
20
0
Quiet
Locomotion
B
Cocktail
ns
SS Frequency (Hz)
140
120
100
80
60
40
20
0
Quiet
Locomotion
C
Control
ns
CS Frequency (Hz)
3
2
1
0
Quiet
Locomotion
D
Cocktail
ns
CS Frequency (Hz)
3
2
1
0
Quiet
Locomotion

Figure 15. Inhibition of noradrenaline has no effect on Z− PC firing activity.

(A) Simple spike activity of Z− PC in control showed no change after 5 min application of adrenergic receptor antagonist cocktail (Control: quiet: 51.75 ± 9.10 Hz, locomotion: 62.34 ± 16.59 Hz; Cocktail: quiet: 56.00 ± 10.69 Hz, locomotion: 71.55 ± 24.86 Hz; mean ± SEM, paired sample t-test, ns; non-significant). (B) Complex spikes showed no difference before or after application of adrenergic receptor antagonist cocktail during behavioral transition (Control: quiet: 1.20 ± 0.11 Hz, locomotion: 1.58 ± 0.32 Hz; Cocktail: quiet: 1.40 ± 0.16 Hz, locomotion: 1.66 ± 0.14 Hz; mean ± SEM, paired sample t-test, ns; non-significant). Recordings of topical application of external solution (control) or adrenergic receptor antagonist cocktail were done in the same cell.

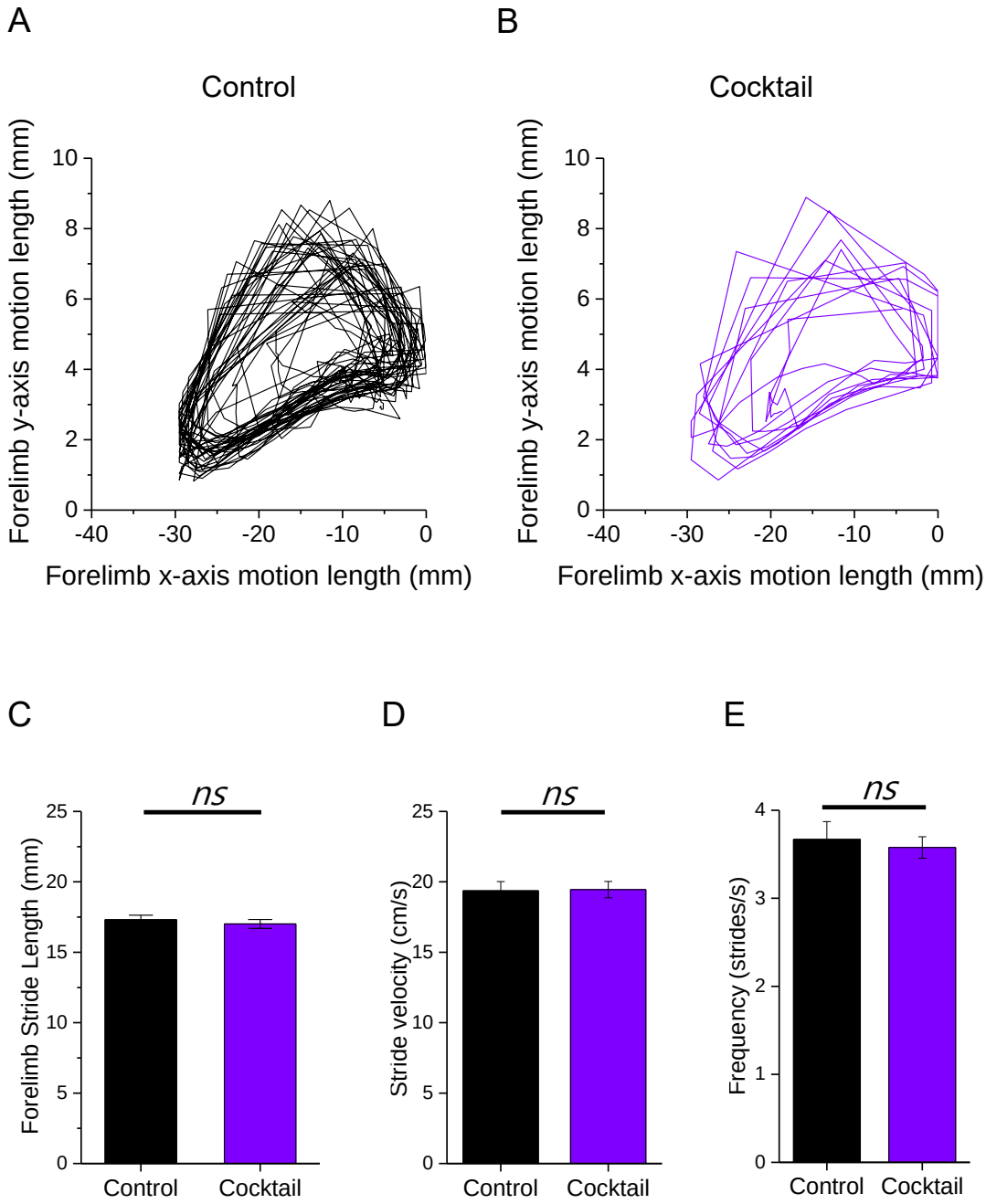
A
Control
Forelimb y-axis motion length (mm)
Forelimb x-axis motion length (mm)
B
Cocktail
Forelimb y-axis motion length (mm)
Forelimb x-axis motion length (mm)
C
ns
Forelimb Stride Length (mm)
Control
Cocktail
D
ns
Stride velocity (cm/s)
Control
Cocktail
E
ns
Frequency (strides/s)
Control
Cocktail

Figure 16. No difference in forelimb motion upon application of adrenergic receptor antagonist cocktail

(A) Representative trace of forelimb motion from external solution applied control mouse. (B) Representative trace of forelimb motion from topically applied adrenergic receptor antagonist cocktail mice. x-axis: stride length; y-axis: vertical movement. (C) Change in forelimb stride motion of control and adrenergic receptor antagonist cocktail applied (n = 6 mice) conditions. Change in forelimb motion under cocktail application show no difference in stride motion (control: stride: 17.3 ± 0.32 mm; Cocktail: stride: 17.015 ± 0.3 mm, mean ± SEM, two-sample t-test, p = 0.51). (D) Velocity of each stride during locomotion. (Control: n = 6 mice, 13 trials, 19.3 ± 0.7 cm/s; Cocktail: n =6, 18 trials, 19.4 ± 0.6 cm/s, mean ± SEM, two-sample t-test, ns; non-significant). (E) Frequency of limb motion during locomotion measured in control and DSP-4 mice (Control: 3.6 ± 0.2 strides/s; Cocktail: 3.6 ± 0.1, mean ± SEM, two-sample t-test, ns; non-significant).

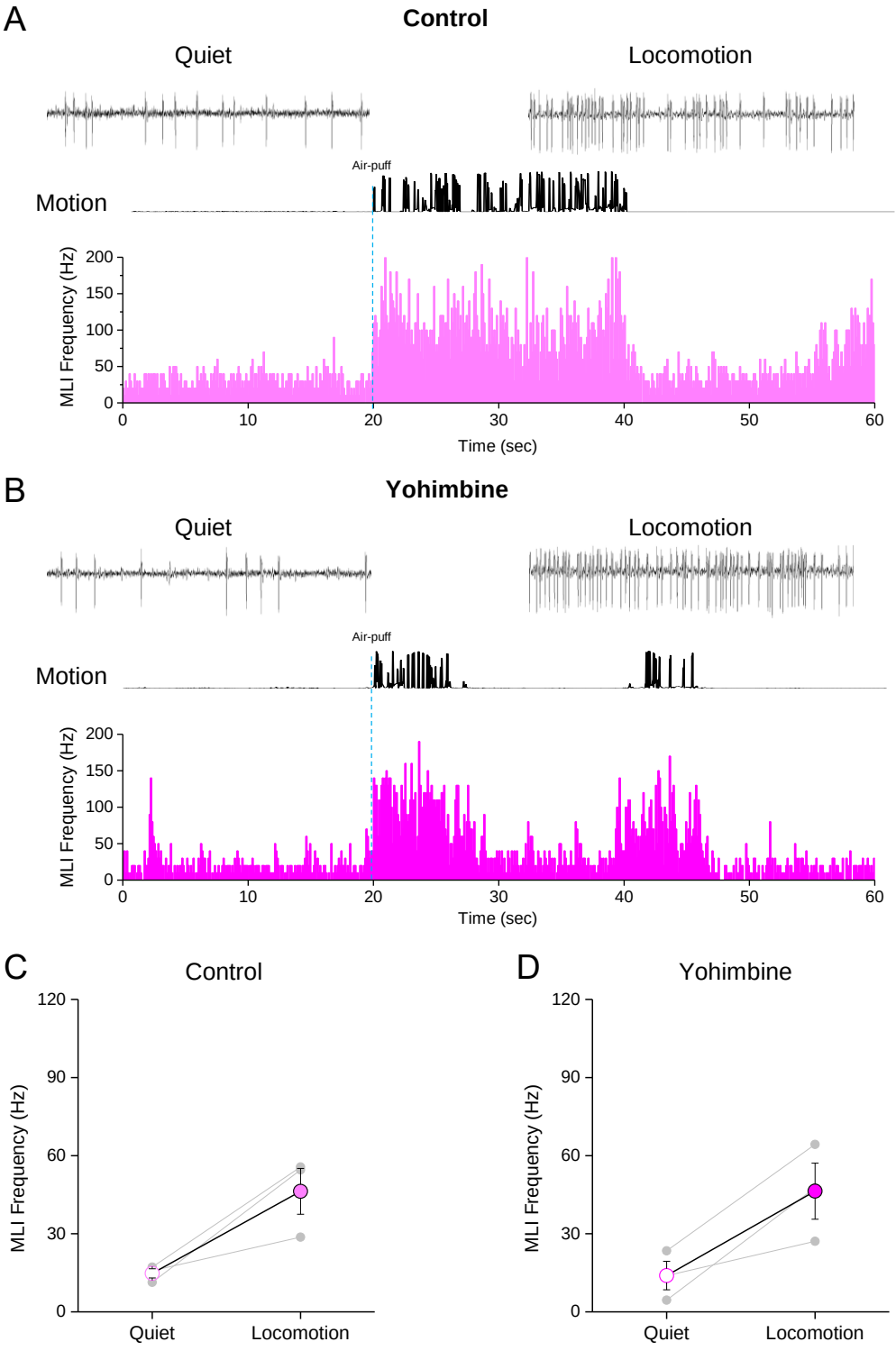
A
Control
Quiet
Locomotion
Air-puff
Motion
MLI Frequency (Hz)
Time (sec)
B
Yohimbine
Quiet
Locomotion
Air-puff
Motion
MLI Frequency (Hz)
Time (sec)
C
Control
MLI Frequency (Hz)
Quiet
Locomotion
D
Yohimbine
MLI Frequency (Hz)
Quiet
Locomotion

Figure 17. Inhibition of α_2-adrenergic receptors on molecular layer interneurons of Z+ modules

(A) Representation of molecular layer interneuron firing activity in Z+ module in saline control condition (light magenta) quiet wakefulness and locomotion shown in peri-stimulus time histogram. Motion index (black) shown in-line with the peri-stimulus time histogram. (B) Molecular layer interneuron spike activity 5 mins after α_2-adrenergic receptor antagonist (yohimbine) application. Peri-stimulus time histogram of molecular layer interneuron activity (magenta) during quiet and locomotion behavioral states. Motion index (black) shown in-line with the peri-stimulus time histogram. (C) Molecular layer interneuron firing activity under control conditions showed increase in firing frequency (control: quiet: 14.8 ± 1.8 Hz, locomotion: 46.3 ± 8.8 Hz, mean ± SEM). (D) Same molecular layer interneuron shown in C after 5 min application of α_2-adrenergic receptor antagonist (Yohimbine: quiet: 13.9 ± 5.5 Hz, locomotion: 46.4 ± 10.8 Hz, mean ± SEM).

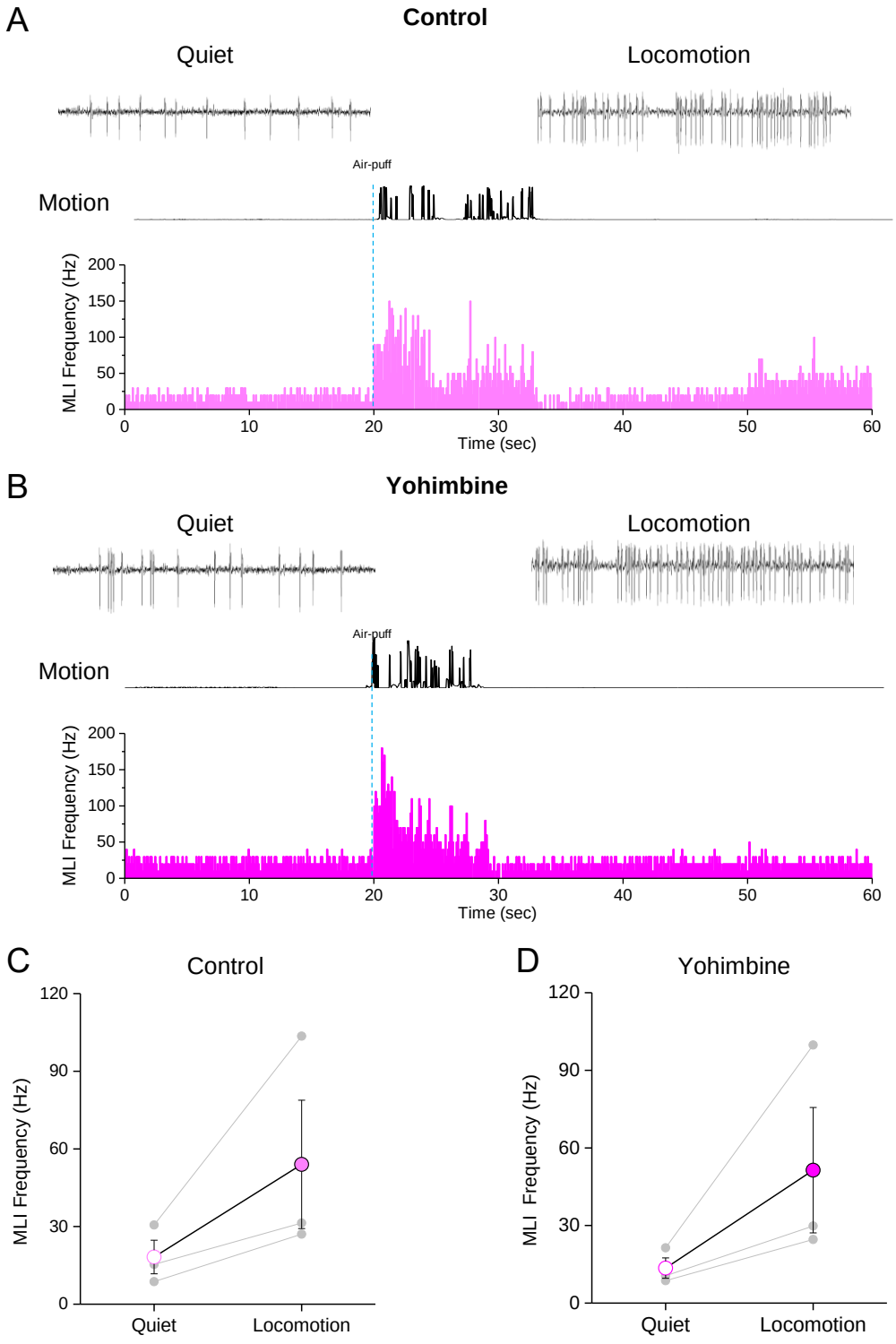
A
Control
Quiet
Locomotion
Air-puff
Motion
MLI Frequency (Hz)
200
150
100
50
0
0
10
20
30
40
50
60
Time (sec)
B
Yohimbine
Quiet
Locomotion
Air-puff
Motion
MLI Frequency (Hz)
200
150
100
50
0
0
10
20
30
40
50
60
Time (sec)
C
Control
MLI Frequency (Hz)
120
90
60
30
0
Quiet
Locomotion
D
Yohimbine
MLI Frequency (Hz)
120
90
60
30
0
Quiet
Locomotion

Figure 18. Inhibition of α_2-adrenergic receptors on molecular layer interneurons of Z− modules

(A) Representation of molecular layer interneuron firing activity in Z− module in control condition (light magenta) quiet wakefulness and locomotion shown in peri-stimulus time histogram. Motion index (black) shown in-line with the peri-stimulus time histogram. (B) Molecular layer interneuron spike activity 5 mins after α_2-adrenergic receptor antagonist (yohimbine) application. Peri-stimulus time histogram of molecular layer interneuron activity (magenta) during quiet and locomotion behavioral states. Motion index (black) shown in-line with the peri-stimulus time histogram. (C) Molecular layer interneuron firing activity under control conditions showed increase in firing frequency (Control: quiet: 18.2 ± 6.5 Hz, locomotion:54 ± 24.8 Hz, mean ± SEM). (D) Same molecular layer interneuron shown in C after 5 min application of α_2-adrenergic receptor antagonist (Yohimbine: quiet: 13.5 ± 4 Hz, locomotion: 51.4 ± 24.2 Hz, mean ± SEM).

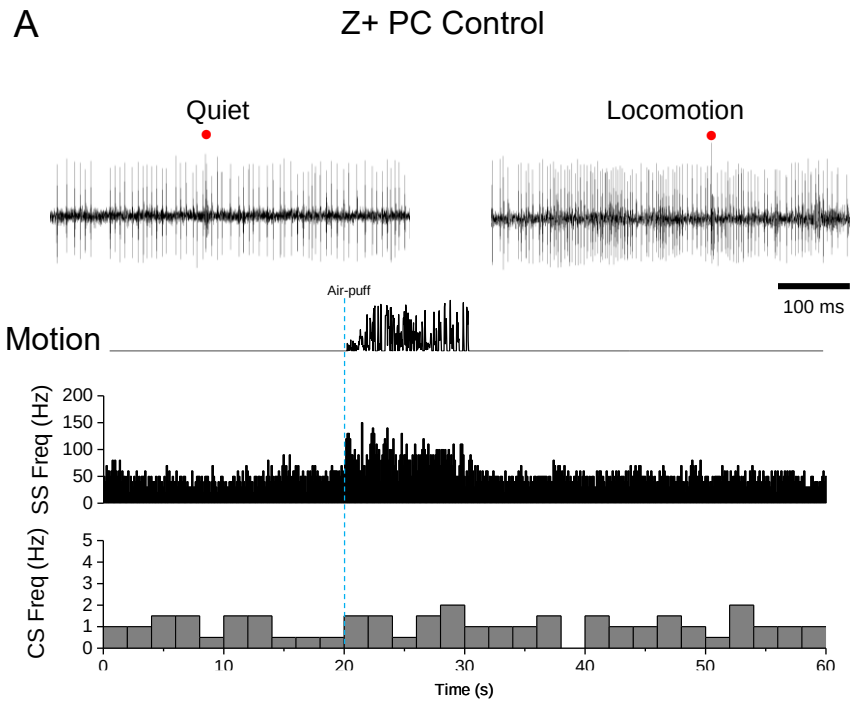
A
Z+ PC Control
Quiet
Locomotion
Air-puff
100 ms
Motion
SS Freq (Hz)
200
150
100
50
0
CS Freq (Hz)
5
4
3
2
1
0
0
10
20
30
40
50
60
Time (s)

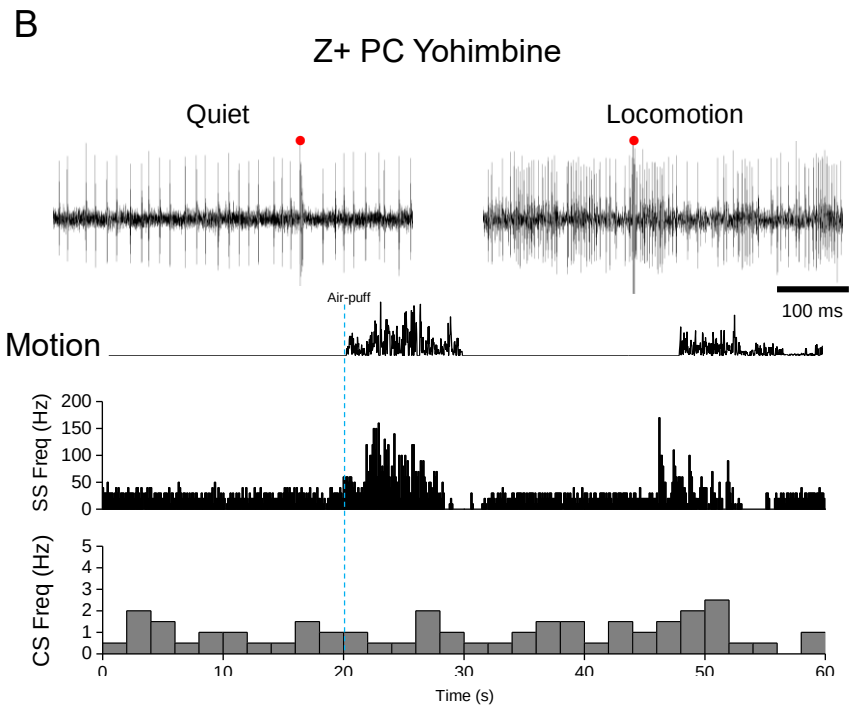
B
Z+ PC Yohimbine
Quiet
Locomotion
Air-puff
100 ms
Motion
SS Freq (Hz)
200
150
100
50
0
CS Freq (Hz)
5
4
3
2
1
0
0
10
20
30
40
50
60
Time (s)

Figure 19. Blockage of α_2- adrenergic receptors during locomotion in Z+ PCs

(A) Representation of simple (black) and complex (grey) spike activity of a Z+ PC in control condition during quiet wakefulness and locomotion shown in peri-stimulus time histogram. Single-unit recordings of Z+ PC(top). Red dot indicates complex spikes. (B) Recording of an identical cell as in (A), 5 mins after α_2-adrenergic receptor antagonist, yohimbine (1mM) application. Peri-stimulus time histogram of simple spike (black) and complex spike (grey) firing during quiet and locomotion behavioral states.

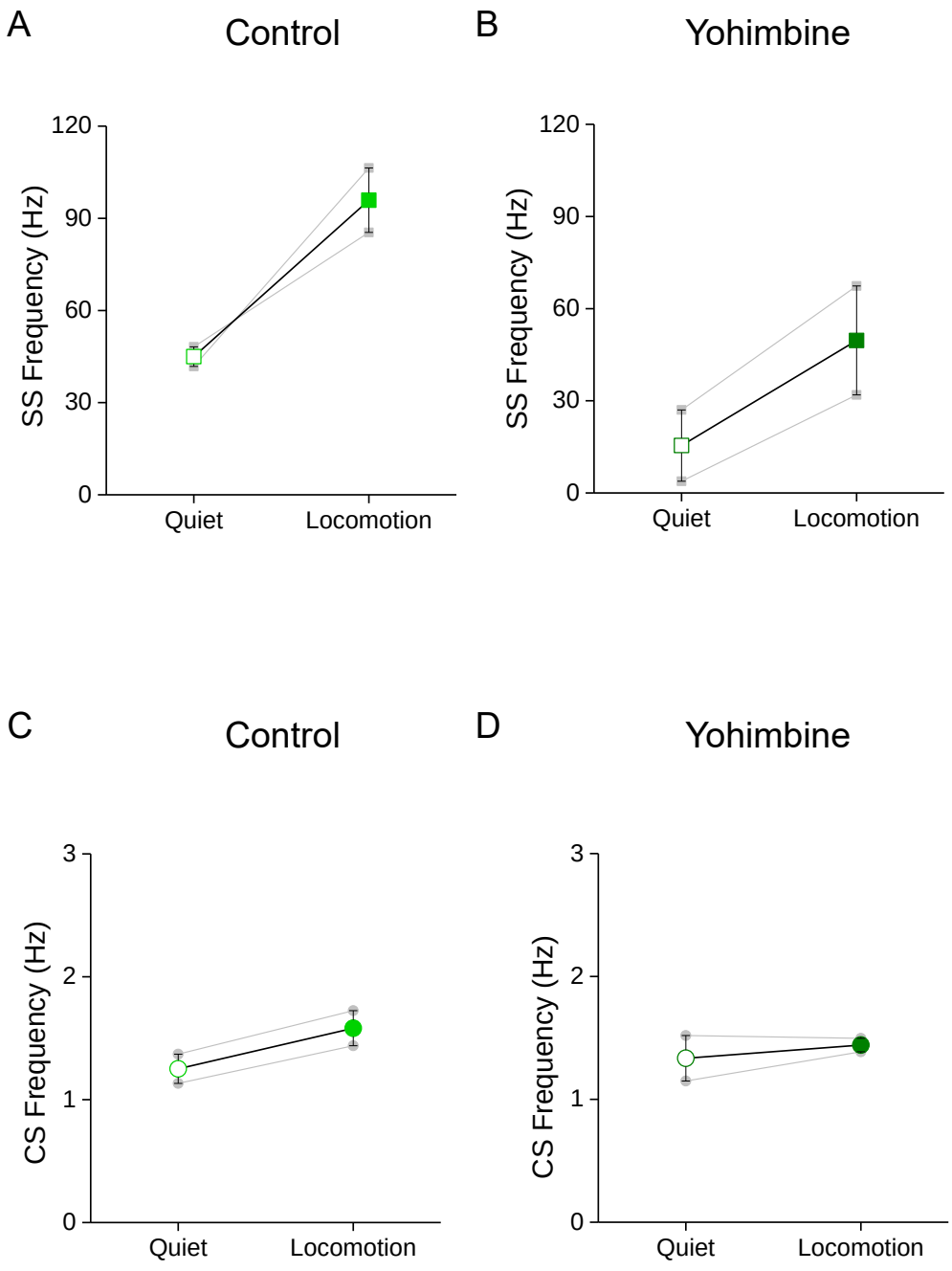
A
Control
B
Yohimbine
SS Frequency (Hz)
120
90
60
30
0
Quiet
Locomotion
C
Control
D
Yohimbine
CS Frequency (Hz)
3
2
1
0
Quiet
Locomotion

Figure 20. Blockage of α_2-adrenergic receptor has no effect on PC simple spike activity

(A) Simple spike activity of Z+ PC in control showed enhancement after 5 min application of yohimbine (1mM) (Control: quiet: 45 ± 3.2 Hz, locomotion: 95.9 ± 10.5 Hz; Cocktail: quiet: 15.4 ± 11.6 Hz, locomotion: 49.6 ± 17.7 Hz; mean ± SEM). (B) Complex spikes showed no difference before or after application of the α_2-adrenergic receptor antagonist during behavioral transition (Control: quiet: 1.25 ± 0.12 Hz, locomotion: 1.58 ± 0.14 Hz; Yohimbine: quiet: 1.33 ± 0.19 Hz, locomotion: 1.44 ± 0.06 Hz; mean ± SEM). Recordings of topical application of external solution (control) or adrenergic receptor antagonist cocktail were done in the same cell.

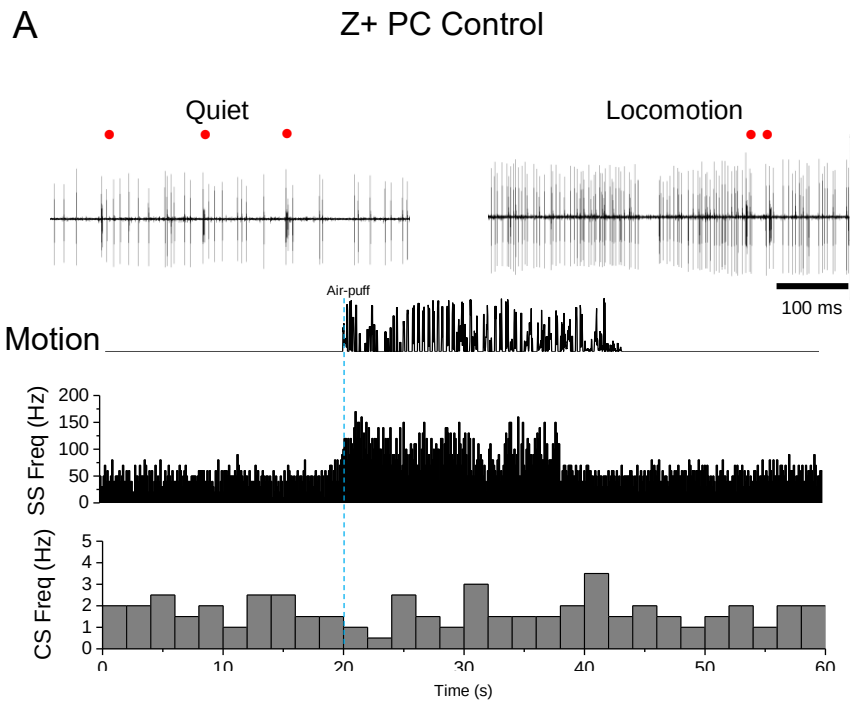
A
Z+ PC Control
Quiet
Locomotion
Air-puff
100 ms
Motion
SS Freq (Hz)
CS Freq (Hz)
Time (s)

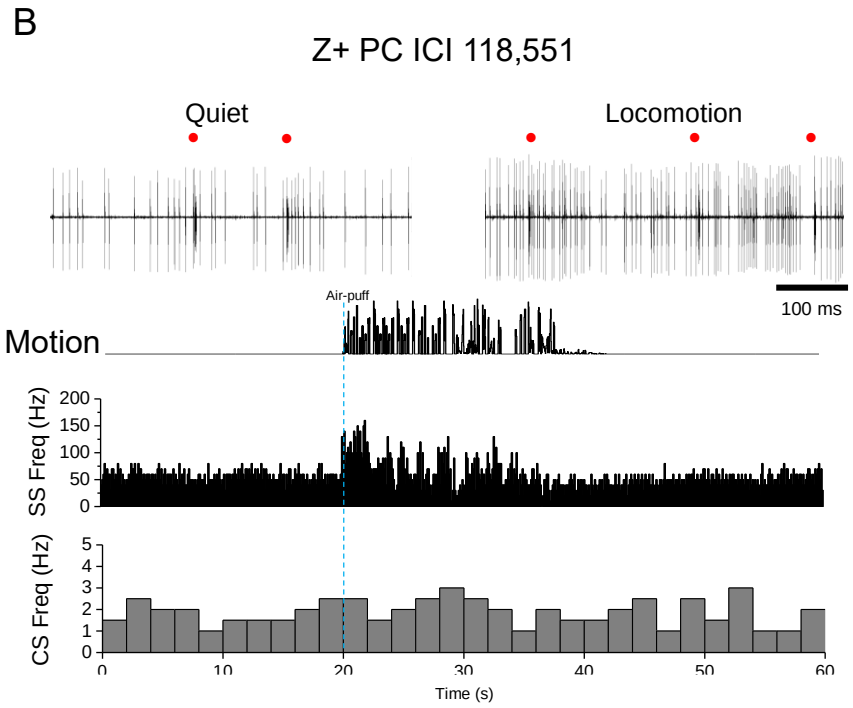
B
Z+ PC ICI 118,551
Quiet
Locomotion
Air-puff
100 ms
Motion
SS Freq (Hz)
CS Freq (Hz)
Time (s)

Figure 21. Effect of β_2-adrenergic receptors by ICI 118, 551 on Z+ PC activity

(A) Representation of Z+ PC activity under control conditions during quiet wakefulness and locomotion state. Red dots indicate complex spikes. Peri-stimulus time histogram of simple spike (black) and complex spike (grey) activity shown with motion index. (B) Identical Z+ PC as in (A) shown under the influence of a β_2-adrenergic receptor antagonist, ICI 118,551 (1 mM).

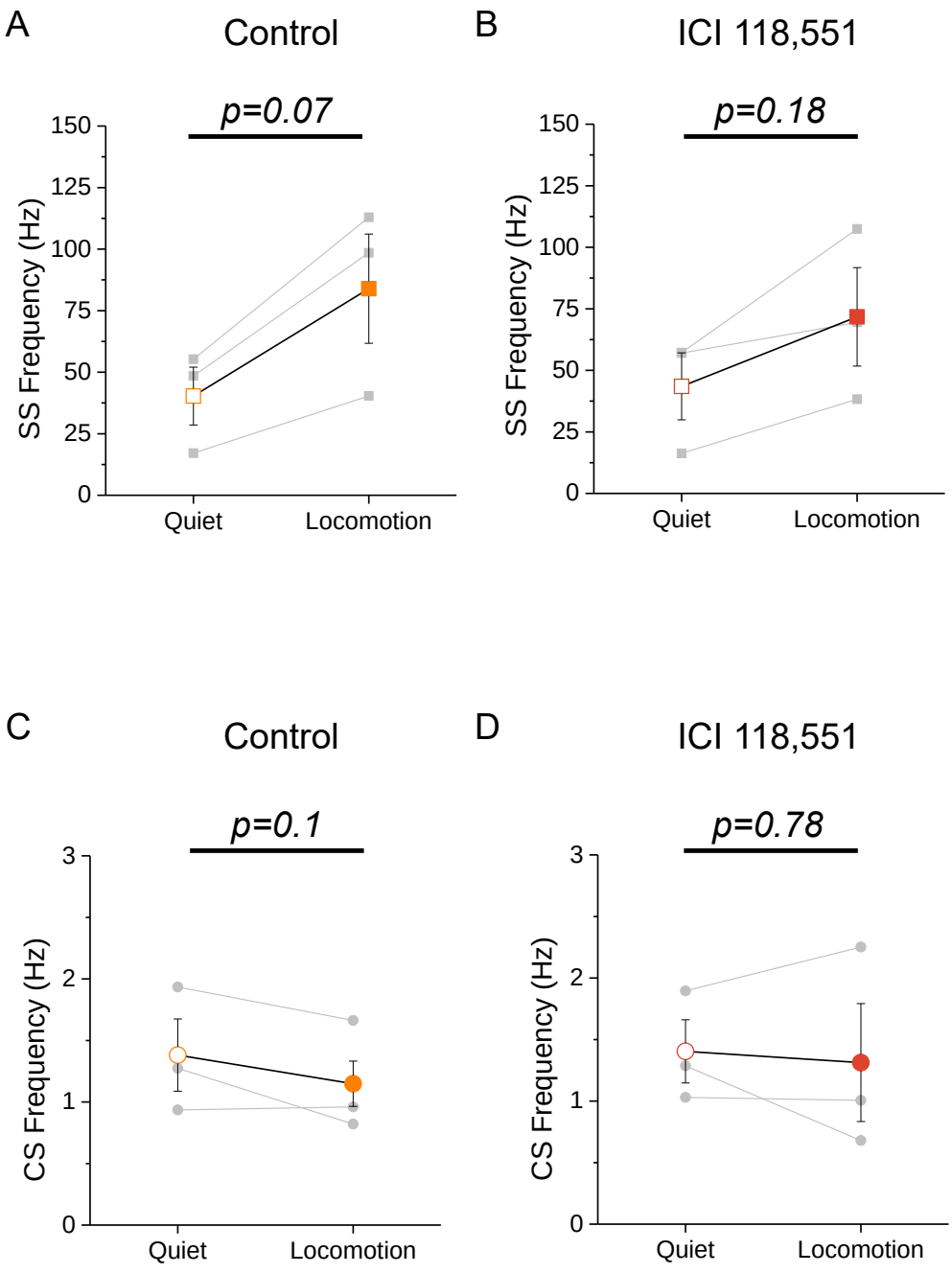
A
Control
p=0.07
SS Frequency (Hz)
150
125
100
75
50
25
0
Quiet
Locomotion
B
ICI 118,551
p=0.18
SS Frequency (Hz)
150
125
100
75
50
25
0
Quiet
Locomotion
C
Control
p=0.1
CS Frequency (Hz)
3
2
1
0
Quiet
Locomotion
D
ICI 118,551
p=0.78
CS Frequency (Hz)
3
2
1
0
Quiet
Locomotion

Figure 22. Inhibition of β_2-adrenergic receptors block enhancement of simple spike activity of Z+ PCs

(A) SS activity under control conditions show an enhancement of SS frequency during locomotion (quiet: 40.3 ± 11.7 Hz, locomotion: 83.9 ± 22.2 Hz, mean ± SEM, paired sample t-test, p =0.07). (B) SS activity under the influence of ICI 118, 551 show decreased enhancement of SS frequency during locomotion (quiet: 43.5 ± 13.6 Hz, locomotion: 71.8 ± 20 Hz, mean ± SEM, paired sample t-test, p = 0.18). (C, D) Complex spike activity during locomotion under control condition or ICI 118, 511 did not show significant change (Control: quiet: 1.38 ± 0.29 Hz, locomotion: 1.15 ± 0.18 Hz, p = 0.1 ; ICI 118, 551: quiet: 1.4 ± 0.26 Hz, locomotion: 1.31 ± 0.48 Hz; mean ± SEM, paired sample t-test, p = 0.78).

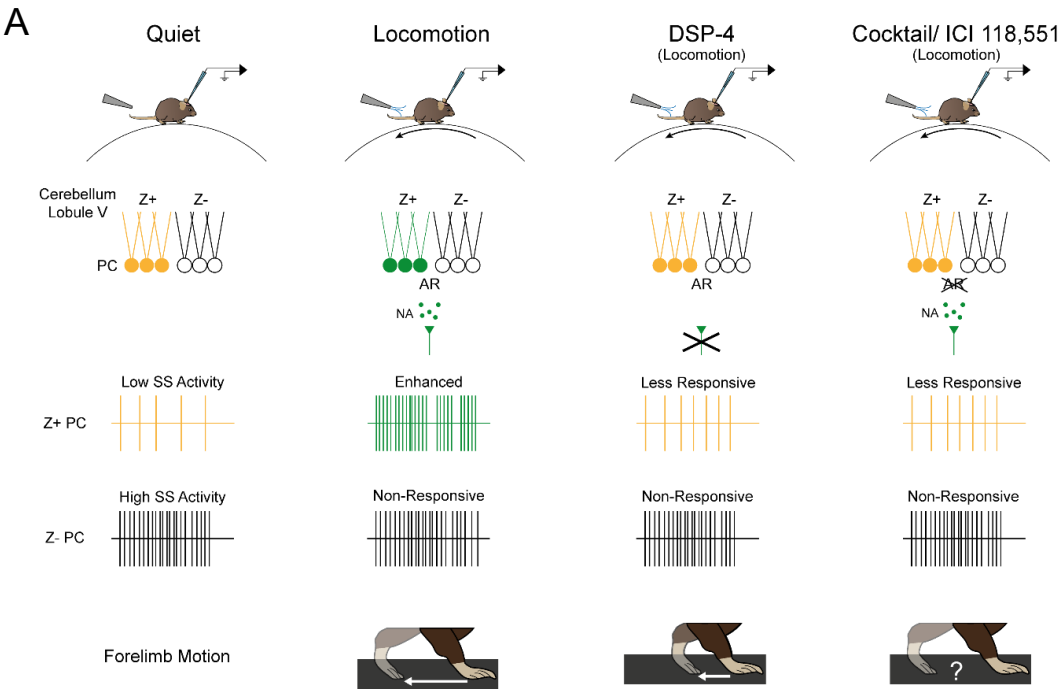
A
Quiet
Locomotion
DSP-4
(Locomotion)
Cocktail/ ICI 118,551
(Locomotion)
Cerebellum
Lobule V
Z+
Z-
PC
AR
NA
Low SS Activity
Enhanced
Less Responsive
Less Responsive
Z+ PC
High SS Activity
Non-Responsive
Non-Responsive
Non-Responsive
Z- PC
Forelimb Motion
?

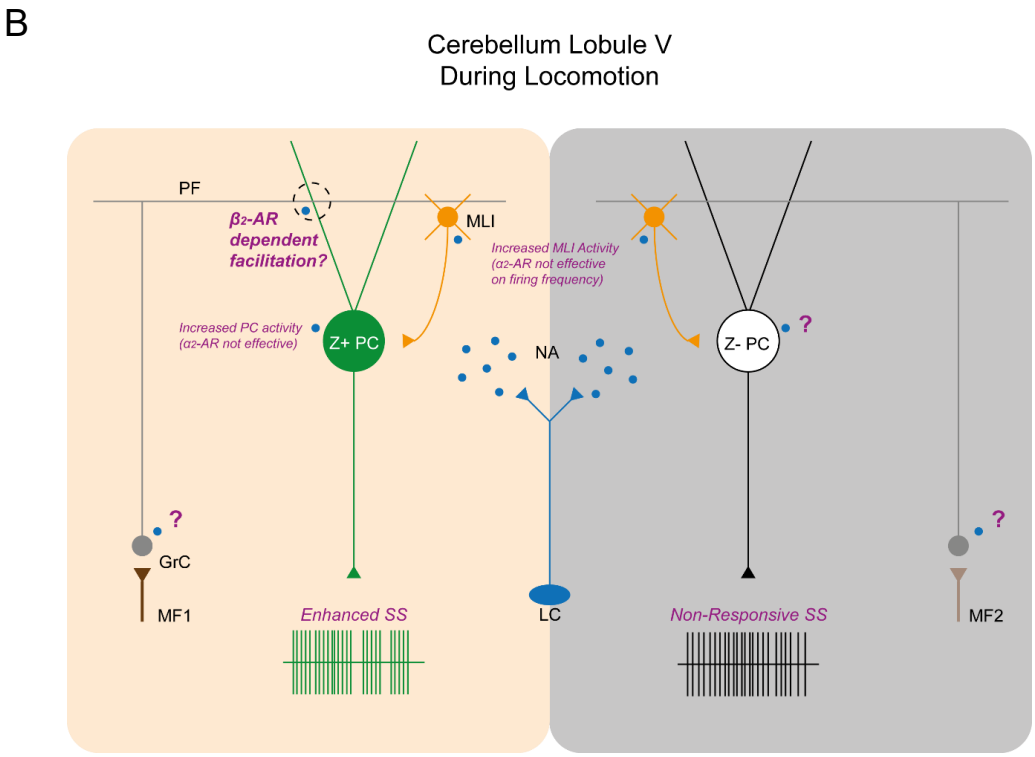
B
Cerebellum Lobule V
During Locomotion
PF
β2-AR
dependent
facilitation?
MLI
Increased MLI Activity
(α2-AR not effective
on firing frequency)
Increased PC activity
(α2-AR not effective)
Z+ PC
NA
Z- PC
?
?
?
GrC
MF1
Enhanced SS
LC
Non-Responsive SS
MF2

Figure 23. Conclusion summary: Noradrenergic effect on zebrin II-dependent PC SS activity and behavior, and its possible mechanisms

(A) Illustration of experimental setup, behavioral state, PC SS activity, and resulting behaviors. During quiet wakefulness state, SS activity of Z+ PCs are low compared to that of Z- PCs. Upon locomotion, SS activity of Z+ PCs are enhanced due to the effect of NA input. Forelimb motion of DSP-4 injected mice show impaired stride lengths while adrenergic receptor antagonist cocktail (cocktail) does not. Further behavioral study of cocktail and β_2-AR antagonist is needed. (B) Possible mechanism for differential modulation of zebrin-dependent PC SS activity during locomotion. Blockage of α_2-AR on MLI or PC does not alter its firing activity during locomotion. However, results imply that β_2-AR expressed on PC may increase the SS activity of PC in Z+ PCs.

Discussion

My data is the first to show in awake behaving mice that differential modulation of PC SS activity is zebrin-dependent and that neuromodulation of NA in the cerebellum is essential for limb motion during locomotion. Although, the function of zebrin II in the cerebellum is not clear, here I show that expression of zebrin show heterogeneity not only in resting state, but also during locomotion motor behavior. My data of differential PC SS firing during locomotion is in line with the previous study of *in vivo* PC recordings in awake mice during locomotion (Jelitai et al., 2016). Interestingly, I found that only Z+ PC SS activity are modulated by NA. Among many adrenergic receptors in the cerebellum, this enhancement of SS in Z+ PCs is caused by β_2-adrenergic receptors on PCs

Differential modulation of PC during locomotion

Bidirectional modulation of PC SS activity has been shown in various studies regarding locomotion (Udo et al., 1981, Armstrong and Edgley, 1984, Edgley and Lidierth, 1988, Armstrong and Edgley, 1988, Jelitai et al., 2016). Also, PCs with different zebrin expression have differences in SS activity during rest (Zhou et al., 2014). I questioned the difference of resting PC firing activity of zebrin modules in the context of motor behavior. My data is the first to discriminate this locomotion-dependent differential modulation by aldolase C/ zebrin II expression. Jelitai et al. (2016) explains that bidirectional

modulation is due to the difference in balance of feedforward excitatory and inhibitory circuit of parallel fibers and molecular layer interneurons on PC output which shapes locomotion-dependent SS bidirectional output. However, they did not take into account of the activation of LC during locomotion, which is the center for noradrenergic output to many brain regions. Although, LC axon terminals are open axon terminals in which only a small amount of synapses are available, NA has been proven to be an important neuromodulator in many brain areas (Spreng et al., 2001, Lahdesmaki et al., 2002, Bekar et al., 2008, Sara, 2009, Ding et al., 2013, Paukert et al., 2014, Schiemann et al., 2015). As shown by my results, not all PCs are modulated by NA. During locomotion, only Z+ PCs increases in SS firing activity while Z− PCs has nearly no apparent response.

NA-dependent in vivo PC activity during locomotion

Many previous reports have shown PC activity decreases upon application of NA or activation of LC-NA circuit (Lippiello et al., 2015, Bickford-Wimer et al., 1991, Guo et al., 2016). However, these reports contradict my results obtained in awake behaving mice in which the effect of NA on PC SS increase with the endogenous secretion of NA during locomotion. This difference in results can be explained by the activity of the granule cells (GCs) during non-locomotive state and locomotive state. Granule cells have been reported to have nearly non-existing activity during quiet wakefulness and only firing during locomotion (Powell et al., 2015, Jelitai et al., 2016). In cerebellar slices or animals under anesthesia, the activity of granule cells is non-

existent due to the absence in mossy fiber input. Thus, the effect of NA on Purkinje cells in slice or anesthetic conditions cannot fully account the effect of NA in awake behaving animals.

PCs receives inhibitory and excitatory inputs via MLIs and GCs, respectively. The balance of excitatory and inhibitory inputs has been shown to regulate the output of the PCs during locomotion (Jelitai et al., 2016). MLIs express α_1 and α_2 adrenergic receptors which dual modulate the activity of the MLI ultimately modulating the inhibitory input to the PC (Hirono and Obata, 2006). Activated α_2 adrenergic receptors lowers the activity of MLIs via inhibition of voltage gated calcium channels and activation of inwardly rectifying K^+ channels. However, my data show that MLI firing activity does not differ upon application of yohimbine, an α_2 adrenergic receptor antagonist (Figure 17 and 18). This may be due to the strong excitatory input of the PFs on the MLIs which occludes the activity of NA on the MLIs.

Granule cells also express α_2 and β_2 adrenergic receptors (Hirono et al., 2008, Lippiello et al., 2015). In the state of locomotion, granule cells may enhance signals of mossy fibers via β_2-AR at mossy fiber-granule cell synapses. However, since granule cells are nearly inactive during the state of quiet wakefulness, it is difficult to identify the cell using single-unit electrophysiological technique. A study have shown that during locomotion a spillover of glutamate at mossy fiber-granule cell synapses, enhances granule cell activity (Powell et al., 2015). Since mossy fibers have been shown to terminate zebrin dependently (Voogd et al., 2003, Pakan et al., 2010), this may be the reason why PCs are differently modulated zebrin-dependently during

locomotion.

One other possible approach to understanding the balance of excitatory and inhibitory input to the output of the cerebellum is to obtain whole-cell recordings of PCs in both modules during locomotion. During locomotion, PCs receive excitatory inputs from PFs of granule cells and inhibitory inputs from MLIs, which also receives input from PFs. By recording the spontaneous excitatory and inhibitory synaptic inputs, I was able to accurately measure the amount of excitatory and inhibitory synaptic inputs which shapes the output of the PCs.

According to Lippiello et al. (2015), β_2 adrenergic receptors potentiate PF-PC synapses by lowering the threshold of potentiation. My results indicate that during locomotion, β_2-ARs are activated to enhance SS firing of Z+ PCs (Figure 21, 22). β_2-AR are also expressed in the granule cell layer. Assuming that β_2-ARs may express in PFs, a presynaptic mechanism may be involved. Due to limited current techniques, it is difficult to isolate the effects of the drug in a cell specific manner. Nevertheless, understanding the effect of NA on the sole output of the cerebellum is important.

NA-dependent limb motion trajectory during locomotion motor behavior

To examine the effects of NA-dependent limb motion, I used motion tracking and analyzed the forelimb motion of the subjects. My data show that injection of DSP-4 disrupted normal forelimb stride motion while local acute

inhibition of cerebellar adrenergic receptors showed no difference in stride motion (Figure 10 and 16). DSP-4 is a global neurotoxin which eliminates noradrenergic terminals throughout the brain (Jonsson et al., 1981, Bekar et al., 2008). Since, normal forelimb motor coordination has been shown to be disrupted by blocking noradrenaline in the motor cortex (Schiemann et al., 2015), the abnormal forelimb stride motion under the influence of DSP-4 may share the similar mechanism. Nevertheless, the effect of DSP-4 affected Z+ PC SS activity during locomotion. Hence, I suspected that there would be a more local effect of the cerebellum to the disordered forelimb motion. Adrenergic antagonist cocktail topically applied on the cerebellum results showed the same electrophysiological properties during locomotion as in DSP-4 injected mice. In spite of the similar SS firing activity upon noradrenaline inhibition, forelimb motion showed no difference in trajectory or stride length.

Cerebellar lobule V of the vermis has been shown to receive limb sensorimotor input (Armstrong and Edgley, 1984, Ozden et al., 2012, Powell et al., 2015). Having roles in monitoring sensorimotor inputs and sending feedback to the muscles, the cerebellum is important in limb coordination. Since, my experimental setup is based on head-fixation, I was not able to see deficits in whole-body balance or stance width, and was only limited to measuring the stride and vertical trajectories. Although that forelimb stride motion had no difference upon blocking adrenergic receptors in lobule V PCs which output during locomotion was impaired (Figure 16), knowing that alteration of PC output impair coordination of limb motion and posture (Hoogland et al., 2015, Machado et al., 2015), a thorough analysis of limb

muscle motion measurement or interlimb coordination is needed.

Implications on Zebrin II-dependent activity during learning

The architecture of the cerebellar cortex has been described by many reviews recently explaining that different protein markers are expressed into parasagittal stripes (Apps and Garwicz, 2005, Apps and Hawkes, 2009, Ruigrok, 2011, Cerminara et al., 2015, Hawkes, 2014). Especially, zebrin II /aldolase C, which the function is unknown is the most-studied marker. Along with expression of zebrin II stripes, many proteins in relation to plasticity are also expressed as parasagittal stripes, such as PLCβ3, PLCβ4, GABABR2, mGluR1β, MAP1A, NCS1, and so on (Cerminara et al., 2015). However, it is not yet well known about how these parasagittal bands differ in terms of plasticity. One study have shown that in accordance to the expression of zebrin II, LTD is easily induced in PF-PC synapses in zebrin II – modules than in zebrin II+ modules(Wadiche and Jahr, 2005). On the other hand, several studies using flavoprotein autofluroescence imaging of the cerebellum show that LTP stimulation of the PF-PC synapses of the cerebellar cortex produce robust LTP and activation coinciding with zebrin II+ stripes (Ebner et al., 2012, Wang et al., 2009). In accordance with my results, SS firing of Z+ PCs were enhanced during locomotion while Z-PCs showed nearly no response. This may be due to the fact that inputs from afferent fibers, such as mossy fiber inputs and climbing fiber inputs, are aligned with PC stripes (Hawkes, 2014). Since I only tested for basic motor behavior, it is unclear how each module will respond in

a learning paradigm. Nonetheless, I was able to observe two different activities for one specific behavior. These results on zebrin dependent activity of PCs may imply the location of LTD and LTP during motor learning.

Association to Noradrenergic Deficiency

The involvement of NA on the cerebellum is crucial for motor behavior. Many diseases such as Parkinson's, Alzheimer's, olivocerebellar atrophy, and Lewy body dementia have been shown to be associated with abnormal NA or adrenergic receptor densities(Kish et al., 1984a, Kish et al., 1984b, Shimohama et al., 1986, Russo-Neustadt and Cotman, 1997, Leverenz et al., 2001, Schambra et al., 2005). In an animal study, NA deficient mice produce a better model for Parkinson's than MPTP, which is commonly used for model Parkinson's disease for its effectiveness to mimic the dopaminergic pathology (Rommelfanger et al., 2007).

Not only is NA important in pathologically, but is it also important in cognition. Various receptor subtypes have been studied to understand its role in learning and memory (Doze et al., 2011, Nalepa et al., 2013, Zhou et al., 2013). Recently, a report suggests the role and mechanism of NA in cerebellar learning (Wakita et al., 2017).

Conclusion

In this study, I investigated the neuromodulatory effect of NA on heterogeneous PCs of zerbin II positive and negative modules and how NA-

dependent PC SS output alters locomotive motor behavior by *in vivo* single-unit recordings and behavioral analysis of forelimb trajectories in awake mice (Figure 23A). My data reveal four main findings. First, I show that modulation of PC SS firing differs during locomotion depending on the expression zebrin II, where SSs of zebrin-positive PCs are enhanced and SSs of zebrin-negative PCs are either non-responsive or decreased during locomotion. Second, enhancement of zebrin-positive PC SS frequency is disrupted via DSP-4, a global neurotoxin which terminates LC neuronal axon terminals, and topical application of adrenergic receptor antagonist cocktail. Third, by motion tracking and analysis, I show that by abolishing the NA-dependent zebrin-positive PC SS output by DSP-4, normal limb motion during locomotion malfunctions. However, no difference in forelimb trajectory was shown in topically applied adrenergic receptor antagonist cocktail conditions and further examination is needed. Finally, I show that the modulation of SS of PCs in zebrin II positive modules are dependent on NA acting on β_2-ARs which enhances the SS firing activity of the zebrin II positive PCs (Figure 23B). Therefore, I conclude that SS firing of cerebellar zebrin II expressing and non-expressing PCs are differentially modulated during locomotion and that the enhancement of SSs of zebrin II expressing PC during locomotor behavior is due to the noradrenergic effect on β_2-adrenergic receptors on PCs.

References

ABBOTT, L. C. & SOTELO, C. 2000. Ultrastructural analysis of catecholaminergic innervation in weaver and normal mouse cerebellar cortices. *J Comp Neurol,* 426**,** 316-29.

APPS, R. & GARWICZ, M. 2005. Anatomical and physiological foundations of cerebellar information processing. *Nat Rev Neurosci,* 6**,** 297-311.

APPS, R. & HAWKES, R. 2009. Cerebellar cortical organization: a one-map hypothesis. *Nat Rev Neurosci,* 10**,** 670-81.

ARMSTRONG, D. M. & EDGLEY, S. A. 1984. Discharges of Purkinje cells in the paravermal part of the cerebellar anterior lobe during locomotion in the cat. *J Physiol,* 352**,** 403-24.

ARMSTRONG, D. M. & EDGLEY, S. A. 1988. Discharges of interpositus and Purkinje cells of the cat cerebellum during locomotion under different conditions. *J Physiol,* 400**,** 425-45.

BARMACK, N. H., QIAN, Z. & YOSHIMURA, J. 2000. Regional and cellular distribution of protein kinase C in rat cerebellar Purkinje cells. *J Comp Neurol,* 427**,** 235-54.

BEKAR, L. K., HE, W. & NEDERGAARD, M. 2008. Locus coeruleus alpha-adrenergic-mediated activation of cortical astrocytes in vivo. *Cereb Cortex,* 18**,** 2789-95.

BICKFORD-WIMER, P., PANG, K., ROSE, G. M. & GERHARDT, G. A. 1991. Electrically-evoked release of norepinephrine in the rat cerebellum: an in vivo electrochemical and electrophysiological study. *Brain Res,* 558**,** 305-11.

BLOOM, F. E., HOFFER, B. J. & SIGGINS, G. R. 1971. Studies on norepinephrine-containing afferents to Purkinje cells of art cerebellum. I. Localization of the fibers and their synapses. *Brain Res,* 25**,** 501-21.

CARTER, M. E., YIZHAR, O., CHIKAHISA, S., NGUYEN, H., ADAMANTIDIS, A., NISHINO, S., DEISSEROTH, K. & DE LECEA, L. 2010. Tuning arousal with optogenetic modulation of locus coeruleus neurons. *Nat*

Neurosci, 13**,** 1526-33.

CERMINARA, N. L., LANG, E. J., SILLITOE, R. V. & APPS, R. 2015. Redefining the cerebellar cortex as an assembly of non-uniform Purkinje cell microcircuits. *Nat Rev Neurosci,* 16**,** 79-93.

CHERICI, C. 2006. Vincenzo Malacarne (1744-1816): a researcher in neurophysiology between anatomophysiology and electrical physiology of the human brain. *C R Biol,* 329**,** 319-29.

CHUNG, S. H., KIM, C. T. & HAWKES, R. 2008. Compartmentation of GABA B receptor2 expression in the mouse cerebellar cortex. *Cerebellum,* 7**,** 295-303.

DEHNES, Y., CHAUDHRY, F. A., ULLENSVANG, K., LEHRE, K. P., STORM-MATHISEN, J. & DANBOLT, N. C. 1998. The glutamate transporter EAAT4 in rat cerebellar Purkinje cells: a glutamate-gated chloride channel concentrated near the synapse in parts of the dendritic membrane facing astroglia. *J Neurosci,* 18**,** 3606-19.

DING, F., O'DONNELL, J., THRANE, A. S., ZEPPENFELD, D., KANG, H., XIE, L., WANG, F. & NEDERGAARD, M. 2013. alpha1-Adrenergic receptors mediate coordinated Ca2+ signaling of cortical astrocytes in awake, behaving mice. *Cell Calcium,* 54**,** 387-94.

DOZE, V. A., PAPAY, R. S., GOLDENSTEIN, B. L., GUPTA, M. K., COLLETTE, K. M., NELSON, B. W., LYONS, M. J., DAVIS, B. A., LUGER, E. J., WOOD, S. G., HASELTON, J. R., SIMPSON, P. C. & PEREZ, D. M. 2011. Long-term alpha1A-adrenergic receptor stimulation improves synaptic plasticity, cognitive function, mood, and longevity. *Mol Pharmacol,* 80**,** 747-58.

EBNER, T. J., WANG, X., GAO, W., CRAMER, S. W. & CHEN, G. 2012. Parasagittal zones in the cerebellar cortex differ in excitability, information processing, and synaptic plasticity. *Cerebellum,* 11**,** 418-9.

EDGLEY, S. A. & LIDIERTH, M. 1988. Step-related discharges of Purkinje cells in the paravermal cortex of the cerebellar anterior lobe in the cat. *J Physiol,* 401**,** 399-415.

ELHADI, A. M., KALB, S., PEREZ-ORRIBO, L., LITTLE, A. S., SPETZLER, R. F. & PREUL, M. C. 2012. The journey of discovering skull base anatomy in ancient Egypt and the special influence of Alexandria. *Neurosurg Focus,* 33**,** E2.

FOOTE, S. L., BLOOM, F. E. & ASTON-JONES, G. 1983. Nucleus locus ceruleus: new evidence of anatomical and physiological specificity. *Physiol Rev,* 63**,** 844-914.

FURUTAMA, D., MORITA, N., TAKANO, R., SEKINE, Y., SADAKATA, T., SHINODA, Y., HAYASHI, K., MISHIMA, Y., MIKOSHIBA, K., HAWKES, R. & FURUICHI, T. 2010. Expression of the IP3R1 promoter-driven nls-lacZ transgene in Purkinje cell parasagittal arrays of developing mouse cerebellum. *J Neurosci Res,* 88**,** 2810-25.

GAO, W., CHEN, G., REINERT, K. C. & EBNER, T. J. 2006. Cerebellar cortical molecular layer inhibition is organized in parasagittal zones. *J Neurosci,* 26**,** 8377-87.

GEBRE, S. A., REEBER, S. L. & SILLITOE, R. V. 2012. Parasagittal compartmentation of cerebellar mossy fibers as revealed by the patterned expression of vesicular glutamate transporters VGLUT1 and VGLUT2. *Brain Struct Funct,* 217**,** 165-80.

GLICKSTEIN, M., STRATA, P. & VOOGD, J. 2009. Cerebellum: history. *Neuroscience,* 162**,** 549-59.

GUO, A., FENG, J. Y., LI, J., DING, N., LI, Y. J., QIU, D. L., PIAO, R. L. & CHU, C. P. 2016. Effects of norepinephrine on spontaneous firing activity of cerebellar Purkinje cells in vivo in mice. *Neurosci Lett,* 629**,** 262-6.

HAWKES, R. 2014. Purkinje cell stripes and long-term depression at the parallel fiber-Purkinje cell synapse. *Front Syst Neurosci,* 8**,** 41.

HIRONO, M., MATSUNAGA, W., CHIMURA, T. & OBATA, K. 2008. Developmental enhancement of alpha2-adrenoceptor-mediated suppression of inhibitory synaptic transmission onto mouse cerebellar Purkinje cells. *Neuroscience,* 156**,** 143-54.

HIRONO, M. & OBATA, K. 2006. Alpha-adrenoceptive dual modulation of inhibitory GABAergic inputs to Purkinje cells in the mouse cerebellum. *J Neurophysiol,* 95**,** 700-8.

HOLMES, G. 1917. The symptoms of acute cerebellar injuries due to gunshot injuries. *Brain,* 40**,** 461-535.

HOOGLAND, T. M., DE GRUIJL, J. R., WITTER, L., CANTO, C. B. & DE ZEEUW, C. I. 2015. Role of Synchronous Activation of Cerebellar Purkinje Cell Ensembles in Multi-joint Movement Control. *Curr Biol,* 25**,** 1157-65.

ILG, W., GIESE, M. A., GIZEWSKI, E. R., SCHOCH, B. & TIMMANN, D. 2008. The influence of focal cerebellar lesions on the control and adaptation of gait. *Brain,* 131**,** 2913-27.

JELITAI, M., PUGGIONI, P., ISHIKAWA, T., RINALDI, A. & DUGUID, I. 2016. Dendritic excitation-inhibition balance shapes cerebellar output during motor behaviour. *Nat Commun,* 7**,** 13722.

JONSSON, G., HALLMAN, H., PONZIO, F. & ROSS, S. 1981. DSP4 (N-(2-chloroethyl)-N-ethyl-2-bromobenzylamine)--a useful denervation tool for central and peripheral noradrenaline neurons. *Eur J Pharmacol,* 72**,** 173-88.

KIEHN, O. 2016. Decoding the organization of spinal circuits that control locomotion. *Nat Rev Neurosci,* 17**,** 224-38.

KISH, S. J., SHANNAK, K. S. & HORNYKIEWICZ, O. 1984a. Reduction of noradrenaline in cerebellum of patients with olivopontocerebellar atrophy. *J Neurochem,* 42**,** 1476-8.

KISH, S. J., SHANNAK, K. S., RAJPUT, A. H., GILBERT, J. J. & HORNYKIEWICZ, O. 1984b. Cerebellar norepinephrine in patients with Parkinson's disease and control subjects. *Arch Neurol,* 41**,** 612-4.

KNAUBER, J. & MULLER, W. E. 2000. Decreased exploratory activity and impaired passive avoidance behaviour in mice deficient for the alpha(1b)-adrenoceptor. *Eur Neuropsychopharmacol,* 10**,** 423-7.

LAHDESMAKI, J., SALLINEN, J., MACDONALD, E., KOBILKA, B. K., FAGERHOLM, V. & SCHEININ, M. 2002. Behavioral and neurochemical characterization of alpha(2A)-adrenergic receptor knockout mice. *Neuroscience,* 113**,** 289-99.

LEVERENZ, J. B., MILLER, M. A., DOBIE, D. J., PESKIND, E. R. & RASKIND, M. A. 2001. Increased alpha 2-adrenergic receptor binding in locus coeruleus projection areas in dementia with Lewy bodies. *Neurobiol Aging,* 22**,** 555-61.

LIPPIELLO, P., HOXHA, E., VOLPICELLI, F., LO DUCA, G., TEMPIA, F. & MINIACI, M. C. 2015. Noradrenergic modulation of the parallel fiber-Purkinje cell synapse in mouse cerebellum. *Neuropharmacology,* 89**,** 33-42.

MACHADO, A. S., DARMOHRAY, D. M., FAYAD, J., MARQUES, H. G. & CAREY, M. R. 2015. A quantitative framework for whole-body coordination

reveals specific deficits in freely walking ataxic mice. *Elife,* 4.

MATEOS, J. M., OSORIO, A., AZKUE, J. J., BENITEZ, R., ELEZGARAI, I., BILBAO, A., DIEZ, J., PUENTE, N., KUHN, R., KNOPFEL, T., HAWKES, R., DONATE-OLIVER, F. & GRANDES, P. 2001. Parasagittal compartmentalization of the metabotropic glutamate receptor mGluR1b in the cerebellar cortex. *Eur. J. Anat.,* 5**,** 15-21.

MISHIMA, K., TANOUE, A., TSUDA, M., HASEBE, N., FUKUE, Y., EGASHIRA, N., TAKANO, Y., KAMIYA, H. O., TSUJIMOTO, G., IWASAKI, K. & FUJIWARA, M. 2004. Characteristics of behavioral abnormalities in alpha1d-adrenoceptors deficient mice. *Behav Brain Res,* 152**,** 365-73.

MORI, S., MATSUI, T., KUZE, B., ASANOME, M., NAKAJIMA, K. & MATSUYAMA, K. 1999. Stimulation of a restricted region in the midline cerebellar white matter evokes coordinated quadrupedal locomotion in the decerebrate cat. *J Neurophysiol,* 82**,** 290-300.

MORTON, S. M. & BASTIAN, A. J. 2007. Mechanisms of cerebellar gait ataxia. *Cerebellum,* 6**,** 79-86.

NALEPA, I., KREINER, G., BIELAWSKI, A., RAFA-ZABLOCKA, K. & ROMAN, A. 2013. alpha1-Adrenergic receptor subtypes in the central nervous system: insights from genetically engineered mouse models. *Pharmacol Rep,* 65**,** 1489-97.

OLSON, L. & FUXE, K. 1971. On the projections from the locus coeruleus noradrealine neurons: the cerebellar innervation. *Brain Res,* 28**,** 165-71.

OZDEN, I., DOMBECK, D. A., HOOGLAND, T. M., TANK, D. W. & WANG, S. S. 2012. Widespread state-dependent shifts in cerebellar activity in locomoting mice. *PLoS One,* 7**,** e42650.

PAKAN, J. M., GRAHAM, D. J. & WYLIE, D. R. 2010. Organization of visual mossy fiber projections and zebrin expression in the pigeon vestibulocerebellum. *J Comp Neurol,* 518**,** 175-98.

PAPAY, R., GAIVIN, R., JHA, A., MCCUNE, D. F., MCGRATH, J. C., RODRIGO, M. C., SIMPSON, P. C., DOZE, V. A. & PEREZ, D. M. 2006. Localization of the mouse alpha1A-adrenergic receptor (AR) in the brain: alpha1AAR is expressed in neurons, GABAergic interneurons, and NG2 oligodendrocyte progenitors. *J Comp Neurol,* 497**,** 209-22.

PAPAY, R., GAIVIN, R., MCCUNE, D. F., RORABAUGH, B. R., MACKLIN, W. B., MCGRATH, J. C. & PEREZ, D. M. 2004. Mouse alpha1B-adrenergic receptor is expressed in neurons and NG2 oligodendrocytes. *J Comp Neurol,* 478**,** 1-10.

PARFITT, K. D., FREEDMAN, R. & BICKFORD-WIMER, P. C. 1988. Electrophysiological effects of locally applied noradrenergic agents at cerebellar Purkinje neurons: receptor specificity. *Brain Res,* 462**,** 242-51.

PAUKERT, M., AGARWAL, A., CHA, J., DOZE, V. A., KANG, J. U. & BERGLES, D. E. 2014. Norepinephrine controls astroglial responsiveness to local circuit activity. *Neuron,* 82**,** 1263-70.

PEARCE, J. M. 2009. Marie-Jean-Pierre Flourens (1794-1867) and cortical localization. *Eur Neurol,* 61**,** 311-4.

PIJPERS, A., WINKELMAN, B. H., BRONSING, R. & RUIGROK, T. J. 2008. Selective impairment of the cerebellar C1 module involved in rat hind limb control reduces step-dependent modulation of cutaneous reflexes. *J Neurosci,* 28**,** 2179-89.

POWELL, K., MATHY, A., DUGUID, I. & HAUSSER, M. 2015. Synaptic representation of locomotion in single cerebellar granule cells. *Elife,* 4.

PURKINYĚ, J. 1837. Bericht die Versammlung deutscher Naturforscher und Ärzte in Prag im September. *Prague. Pt,* 3.

QUY, P. N., FUJITA, H., SAKAMOTO, Y., NA, J. & SUGIHARA, I. 2011. Projection patterns of single mossy fiber axons originating from the dorsal column nuclei mapped on the aldolase C compartments in the rat cerebellar cortex. *J Comp Neurol,* 519**,** 874-99.

RAM N Y CAJAL, S. & AZOULAY, L. 1909. *Histologie du système nerveux de l'homme & des vertébrés,* Paris, A. Maloine.

ROMMELFANGER, K. S., EDWARDS, G. L., FREEMAN, K. G., LILES, L. C., MILLER, G. W. & WEINSHENKER, D. 2007. Norepinephrine loss produces more profound motor deficits than MPTP treatment in mice. *Proc Natl Acad Sci U S A,* 104**,** 13804-9.

ROSS, S. B. & STENFORS, C. 2015. DSP4, a selective neurotoxin for the locus coeruleus noradrenergic system. A review of its mode of action.

Neurotox Res, 27**,** 15-30.

RUIGROK, T. J. 2011. Ins and outs of cerebellar modules. *Cerebellum,* 10**,** 464-74.

RUSSO-NEUSTADT, A. & COTMAN, C. W. 1997. Adrenergic receptors in Alzheimer's disease brain: selective increases in the cerebella of aggressive patients. *J Neurosci,* 17**,** 5573-80.

SAITOW, F., SUZUKI, H. & KONISHI, S. 2005. beta-Adrenoceptor-mediated long-term up-regulation of the release machinery at rat cerebellar GABAergic synapses. *J Physiol,* 565**,** 487-502.

SARA, S. J. 2009. The locus coeruleus and noradrenergic modulation of cognition. *Nat Rev Neurosci,* 10**,** 211-23.

SARNA, J. R., MARZBAN, H., WATANABE, M. & HAWKES, R. 2006. Complementary stripes of phospholipase Cbeta3 and Cbeta4 expression by Purkinje cell subsets in the mouse cerebellum. *J Comp Neurol,* 496**,** 303-13.

SAUERBREI, B. A., LUBENOV, E. V. & SIAPAS, A. G. 2015. Structured Variability in Purkinje Cell Activity during Locomotion. *Neuron,* 87**,** 840-52.

SCHAMBRA, U. B., MACKENSEN, G. B., STAFFORD-SMITH, M., HAINES, D. E. & SCHWINN, D. A. 2005. Neuron specific alpha-adrenergic receptor expression in human cerebellum: implications for emerging cerebellar roles in neurologic disease. *Neuroscience,* 135**,** 507-23.

SCHIEMANN, J., PUGGIONI, P., DACRE, J., PELKO, M., DOMANSKI, A., VAN ROSSUM, M. C. & DUGUID, I. 2015. Cellular mechanisms underlying behavioral state-dependent bidirectional modulation of motor cortex output. *Cell Rep,* 11**,** 1319-30.

SCHWARZ, L. A. & LUO, L. 2015. Organization of the locus coeruleus-norepinephrine system. *Curr Biol,* 25**,** R1051-6.

SHIMOHAMA, S., TANIGUCHI, T., FUJIWARA, M. & KAMEYAMA, M. 1986. Biochemical characterization of alpha-adrenergic receptors in human brain and changes in Alzheimer-type dementia. *J Neurochem,* 47**,** 1295-301.

SHIN, S. L., HOEBEEK, F. E., SCHONEWILLE, M., DE ZEEUW, C. I., AERTSEN, A. & DE SCHUTTER, E. 2007. Regular patterns in cerebellar Purkinje cell simple spike trains. *PLoS One,* 2**,** e485.

SKALHEGG, B. S. & TASKEN, K. 2000. Specificity in the cAMP/PKA signaling pathway. Differential expression,regulation, and subcellular localization of subunits of PKA. *Front Biosci,* 5**,** D678-93.

SPRENG, M., COTECCHIA, S. & SCHENK, F. 2001. A behavioral study of alpha-1b adrenergic receptor knockout mice: increased reaction to novelty and selectively reduced learning capacities. *Neurobiol Learn Mem,* 75**,** 214-29.

SUGIYAMA, D., HUR, S. W., PICKERING, A. E., KASE, D., KIM, S. J., KAWAMATA, M., IMOTO, K. & FURUE, H. 2012. In vivo patch-clamp recording from locus coeruleus neurones in the rat brainstem. *J Physiol,* 590**,** 2225-31.

TAYLOR, S. S., ILOUZ, R., ZHANG, P. & KORNEV, A. P. 2012. Assembly of allosteric macromolecular switches: lessons from PKA. *Nat Rev Mol Cell Biol,* 13**,** 646-58.

THACH, W. T., GOODKIN, H. P. & KEATING, J. G. 1992. The cerebellum and the adaptive coordination of movement. *Annu Rev Neurosci,* 15**,** 403-42.

UDO, M., MATSUKAWA, K., KAMEI, H., MINODA, K. & ODA, Y. 1981. Simple and complex spike activities of Purkinje cells during locomotion in the cerebellar vermal zones of decerebrate cats. *Exp Brain Res,* 41**,** 292-300.

VOOGD, J., PARDOE, J., RUIGROK, T. J. & APPS, R. 2003. The distribution of climbing and mossy fiber collateral branches from the copula pyramidis and the paramedian lobule: congruence of climbing fiber cortical zones and the pattern of zebrin banding within the rat cerebellum. *J Neurosci,* 23**,** 4645-56.

WADICHE, J. I. & JAHR, C. E. 2005. Patterned expression of Purkinje cell glutamate transporters controls synaptic plasticity. *Nat Neurosci,* 8**,** 1329-34.

WAKITA, R., TANABE, S., TABEI, K., FUNAKI, A., INOSHITA, T. & HIRANO, T. 2017. Differential regulations of vestibulo-ocular reflex and optokinetic response by beta- and alpha2-adrenergic receptors in the cerebellar flocculus. *Sci Rep,* 7**,** 3944.

WANG, X., CHEN, G., GAO, W. & EBNER, T. 2009. Long-term potentiation of

the responses to parallel fiber stimulation in mouse cerebellar cortex in vivo. *Neuroscience,* 162**,** 713-22.

WELSH, J. P., LANG, E. J., SUGLHARA, I. & LLINAS, R. 1995. Dynamic organization of motor control within the olivocerebellar system. *Nature,* 374**,** 453-7.

ZHOU, H., LIN, Z., VOGES, K., JU, C., GAO, Z., BOSMAN, L. W., RUIGROK, T. J., HOEBEEK, F. E., DE ZEEUW, C. I. & SCHONEWILLE, M. 2014. Cerebellar modules operate at different frequencies. *Elife,* 3**,** e02536.

ZHOU, H. C., SUN, Y. Y., CAI, W., HE, X. T., YI, F., LI, B. M. & ZHANG, X. H. 2013. Activation of beta2-adrenoceptor enhances synaptic potentiation and behavioral memory via cAMP-PKA signaling in the medial prefrontal cortex of rats. *Learn Mem,* 20**,** 274-84.

국문 초록

소뇌는 보폭, 팔다리의 궤적, 균형 같은 운동 조절을 유지하는데 있어서 중요한 역할을 한다. 그 중 퍼킨지 세포가 소뇌의 최종 출력으로써 중요한 역할을 갖는다. 모든 퍼킨지 세포는 단일 형상으로 되어있지만 실제로는 zebrin II를 기준으로 서로 다른 단백질과 전기생리학적 성격을 지니는 모듈로 나눠져있다. 퍼킨지 세포가 받는 국소적인 시냅스 입력외에도 청반으로부터 유래하는 노아드레날린 입력이 있다. 청반-노아드레날린 회로는 운동시 활성화 되고 소뇌로 노아드레날린이 분비 된다. 그러나 노아드레날린이 퍼킨지 세포의 출력에 어떻게 기여하며 그것이 운동에 어떻게 영향을 주는지는 해결되지 않았다. 본 연구에서는 깨어있는 행동가능한 마우스에서 *in vivo* single-unit 기록을 통하여 퍼킨지 세포를 기록하여 약리학적 접근과 행동 분석을 통하여 노아드레날린이 퍼킨지 세포를 zebrin II 모듈간에 어떻게 조절하고 있는지를 연구하였다. 실험 결과, zebrin II를 발현하고 있는 퍼킨지 세포는 운동시에 단순가시전압 (simple spike) 활성도가 증가 하였고, zebrin II를 발현 하고 있지 않은 퍼킨지 세포들은 운동시에 반응하지 않거나 감소하는 세포들이 있었다. 이렇게 운동시 상이하게 반응하는 각 zebrin II 모듈은 DSP-4 약물주입을 통해서 노아드레날린 축삭 말단을 약물로 파괴하거나 아드레날린 수용체 길항제 혼합액을 통해 소뇌내의 수용체를 국소적으로 직접 막거나 했을 때에 운동시에 단순 가시전압이 반응하지 않는 것으로

확인 되었다. 그러나 행동 분석 결과는 노아드레날린의 영향을 DSP-4를 통해 막았을 때에만 앞다리의 보폭의 차이가 나고 아드레날린 수용체 길항제 혼합핵을 주었을 때는 차이가 안나는 것으로 나타났다. 운동시 Zebrin II 발현하고 있는 퍼킨지 세포의 단순가시전압의 증가의 기전을 보고자 α_2-아드레날린 수용체가 분자층 중간 뉴런(molecular layer interneuron)의 활성에 미치는 영향을 보았다. α_1와 α_2-아드레날린 수용체를 갖고 있는 분자층 중간 뉴런은 기존 in vitro 실험 결과에서 양방향적으로 분자층 중간 뉴런의 활성도를 조절한다고 보고했다. 분자층 중간 뉴런을 in vivo에서 기록한 결과 운동시 모든 모듈의 분자층 중간 뉴런의 활성도는 통제군과 비교하여 α_2-아드레날린 수용체를 막았을 때에도 변하지 않았다. 그 다음으로는 퍼킨지 세포에 있는 수용체의 영향을 보고자 하였다. α_2-아드레날린 수용체 억제시 통제군과 동일하게 운동시에 증가 하였지만, β_2-아드레날린 수용체 억제시에는 단순가시전압의 활성도를 감소 시키는 경향성을 보였다. 결론적으로 본 연구 결과는 노아드레날린은 소뇌에서 아마도 β_2-아드레날린 수용체를 통한 신경조절 물질로 작용하여 zebrin II을 발현하고 있는 퍼킨지 세포의 단순가시전압 출력을 조절함을 제시한다.

주요어: 소뇌, 노아드레날린, 퍼킨지 세포, 제브린, 단순가시전압 활성, 운동

학 번: 2009 – 21857